THREE ESSAYS ON CO-MOVEMENT IN FINANCIAL MARKET: FRACTAL BEHAVIOR, INFORMATION FLOW, CAUSALITY AND FORECASTING

CENGİZ KARATAŞ

JUNE, 2022

THREE ESSAYS ON CO-MOVEMENT IN FINANCIAL MARKET: FRACTAL BEHAVIOR, INFORMATION FLOW, CAUSALITY AND FORECASTING

BY

CENGİZ KARATAŞ

DISSERTATION SUBMITTED IN PARTIAL FULFILLMENT

OF THE REQUIREMENTS FOR THE DEGREE OF DOCTOR OF PHILOSOPHY

IN

DEPARTMENT OF FINANCIAL ECONOMICS

YEDITEPE UNIVERSITY

JUNE, 2022

PLAGIARISM

I hereby declare that all information in this document has been obtained and presented in accordance with academic rules and ethical conduct. I also declare that, as required by these rules and conduct, I have fully cited and referenced all material and results that are not original to this work.

30.06.2022

CENGİZ KARATAŞ

ABSTRACT

The behavior of financial time series, their interactions with each other, and analyzes of forecasts especially in crisis and shock periods, have gained an important place in the literature. In the coming years, such analyzes will find a place in many studies. The relationships between financial time series are a very important indicator in analyzing the economic shocks encountered. There are many methodologies and analyses on this subject in the literature. From this point of view, the aim of the thesis is to analyze the co-movement of financial time series, fractal behavior, the measure and direction of information flow, and future price forecasting, and to develop new analysis methods. The fact that all these methods have not been studied together is another starting point of the thesis. In the first part of the thesis, the co-movement of financial time series was analyzed by Wavelet coherence (WTC) method, crisis and shock periods were determined by Multiple wavelet coherence (MWC) method, then fractal behaviors were examined with Multifractal de-trended fluctuation analysis (MFDFA) method and for the post-crisis periods, daily price range estimations for the future were made by using the Vector autoregressive fractionally integrated moving average (VARFIMA) method, in comparison with real data. In the second part, a new method called Wavelet transform guided transfer entropy method (WTGTEM) has been proposed. In this new method, the co-movement of exchange rate time series has been examined with the Wavelet coherence (WTC) method, and the measurement and direction of the information flow between the financial series under the guidance of WTC have been analyzed by the Transfer entropy (TE) method. In the last part of the thesis, the new methodology presented in the second part has been applied to major stock indices. Especially during

the COVID period, the behavior of the series has been analyzed, and it would be helpful for investors in portfolio diversification, especially in times of crisis. We believe that this thesis will guide future studies of this kind and that the methods used will be preferred by researchers.

ÖZET

Özellikle kriz ve şok dönemlerinde finansal zaman serilerinin davranışları, birbirleri ile olan etkileşimleri ve ileriye dönük tahminlerinin analizleri literatürde önemli bir yer edinmiştir. Gelecek yıllarda da bu tür analizler birçok çalışmada yer bulacaktır. Finansal zaman serilerinin birbiri arasındaki ilişkiler, karşılaşılan ekonomik şokları analiz etmede çok önemli bir göstergedir. Literatürde bu konu ile ilgili birçok metodoloji ve analiz mevcuttur. Buradan hareketle tezin amacı finansal zaman serilerinin birlikte hareketinin, fractal davranışlarının, bilgi akışının ölçümünün ve yönünün tespiti ve geleceğe dönük fiyat tahmini analizlerinin yapılması ve analiz yöntemlerinin geliştirilmesidir. Tüm bu yöntemlerin birlikte çalışılmamış olması da tezin bir başka çıkış noktasıdır. Tezin birinci bölümünde, finansal zaman serilerin birlikte hareketi Dalgacık uyumu (WTC) metodu ile analiz edilmiş, Çoklu dalgacık uyumu (MWC) yöntemi kriz ve şok dönemleri tespit edilmiş, daha sonra Çoklu fractal meyilden arındırılmış dalgalanma analizi (MFDFA) metodu ile fractal davranışaları incelenmiş, kriz sonrası dönemlere yönelik Vektörel özbağlanımlı fraksiyonlu bütünleşmiş hareketli ortalama (VARFIMA) yöntemi ile gerçek data ile karşılaştırılmalı olarak geleceğe yönelik günlük fiyat aralığı tahminleri yapılmıştır. İkinci bölümde Dalgacık dönüşümü kılavuzlu transfer entropi yöntemi (WTGTEM) adında yeni bir metod ileri sürülmüştür. Bu yöntem de, döviz kuru zaman serilerinin birlikte hareketi Dalgacık uyumu (WTC) metodu ile incelenmiş ve WTC rehberliğinde finansal serilerinin birbirleri arasındaki bilgi akışının ölçümü ve yönü Transfer entropi (TE) yöntemi ile analiz edilmiştir. Tezin son bölümünde ise ikinci bölümde sunulan yeni metodoloji major stock endekslerine uygulanmıştır. Özellikle COVID döneminde serilerin davranışları analiz edilmiştir. Yatırımcılar için özelllikle kriz

dönemlerinde potfolio çeşitlemesi için yardımcı olacağı gösterilmiştir. Bu tezin, bundan sonra yapılacak bu tür çalışmalara rehberlik edeceği ve özellikle kullanılan methodların araştırmacılar için tercih edileceği düşüncesindeyiz.

Too my wife Burcu Karataş, my family and

my dear supervisor Prof. Dr. Gazanfer Ünal,

who passed away a short time ago.

ACKNOWLEDGMENT

First of all, I would like to express my endless respect and gratitude to my previous thesis advisor, my dear teacher Prof. Dr. Gazanfer Ünal, who recently passed away, who guided me to this study, and made great contributions in the field of finance and economics, and contributed greatly to the development of the thesis. I will continue my academic career on the path he opened for me, always with gratitude and longing for him.

I would also like to express my deep gratitude to my supervisor, Prof. Dr. Veysel Ulusoy, for all his contributions to me in the fields of finance and economics and for all his efforts to advance my career.

I would like to thank dear my lecturers on my thesis committee Prof. Dr. Ahmet Özçam and Assoc. Dr. Sema Dube.

I would like to thank my dear friends Ebru Kılıç, Melike Akça, Gülşah Alcan, Adil Yılmaz, Itır Doğangün and Tunç Oygur for their support and friendship.

I also would like to thank my wife Burcu Karataş and my family for their endless support for all my life.

TABLE OF CONTENTS

LIST OF TABLES

LIST OF FIGURES

CHAPTER 1: CO-MOVEMENT, FRACTAL BEHAVIOUR AND FORECASTING OF EXCHANGE RATES

Summary

In this chapter, we analyze the fractal behavior and correlations of exchange rates and develop a new approach to obtain better forecast results with small errors. Multifractal de-trended fluctuation analysis (MFDFA) is used to get fractal time series and their Hurst Exponents in the specific time period and based on these results. We established Vector autoregressive fractionally integrated moving average (VARFIMA) models of exchange rates on certain dates. Hurst Exponents (H) allows us to detect small fluctuations (persistent characteristic) of time series and their multifractal behavior. We consider USD/CAD, USD/GBP, USD/EUR, and USD/CHF exchange rates as time series. Our theory is to show that if a time series has the highest multifractal degree, then it has the most successful prediction results for the time interval in which four-time series have the highest co-movement. We use Wavelet coherence (WTC) analysis to understand the co-movement of the exchange rates. The findings of Wavelet Coherence showed co-movement between these exchange rates, the relationships among the two and four rates (with multiple wavelet coherence-MWC), and how these connections differ in the space of frequency-time. These relations and MFDFA results authorize us to construct VARFIMA models of exchange rate data which produce effective forecast outcomes with small errors.

1.1. Introduction

The exchange rate is the value of a nation's currency in the form of a foreign currency. We used daily prices of currency values for daily co-movements among exchange rate values. After the shocks that occur during financial crisis periods, an increase in one exchange rate affects the other rates. We want to show the relationship between these rates and fractal behavior of exchange rate by the mathematical processes, the co-movement between two exchange rates by WTC, four rates by MWC, and detecting whether a time series has long memory or not by MFDFA.

Analysis of wavelets helps us to discern co-movement between time series. While there are several analyses, wavelet analysis differentiates by expanding the frequency and time domain, most specifically Fourier analysis, for this reason. It then enables one to analyze co-movements in detail in both domains. As a result of these characteristics, the wavelet approach proposes broad research areas that vary through geophysics to biomedicine.

The works of Torrence and Compo (1998) accelerated quantitative performance in wavelet analysis applications in particular. They established new statistically significant measures by defining significance rates and confidence intervals and defining coherence, and cross-wavelet spectra focused on atmospheric data series in their research.

Grinsted et al. (2004) extended WTC and cross wavelet transformation applications for two-time series, concentrating on wavelet analysis. Using extended wavelet software methods for geophysical time series, they have demonstrated the use of phase angle statistics to test confidence in causative relationships.

Via cross-wavelet study, Tiwari (2012) researched the correlations among share prices and interest rates in the Indian economy and inflation, industrial output, and oil prices in the German economy. Barunik et al. (2012), (2013) look at the traded assets co-movements such as stocks, oil and gold, European stock markets, and energy commodities, test time-frequency dynamics, and contrast findings with traditional econometric instruments.

A recent field of mathematics, fractal geometry, was founded in the 1960 and 1970s via Benoit Mandelbrot (1977), which has been proven helpful in modeling various dynamic, chaotic phenomena of nature. In recent years, several artifacts of human derivation have been found, such as network traffic dynamics (W. Willinger et al., 1994), and the stock market (E.E. Peters, 1994) as well as (B. Mandelbrot et al., 1997) show fractal qualities.

Barunik et al. (2012) performed a comprehensive survey using the Markov switching multifractal (MSM) theory to describe the multifractal characteristics of various financial series (US treasury bond prices, USD/GBP and USD/EUR exchange rates, Nikkei and Dow Jones price indices). They demonstrate that the fat-tailed distributional property of the financial series is a central multifractality element.

The latest study about multifractality in exchange rate returns by Günay (2014) without recognize the co-movement. He noted that there is a high presence of multifractality in USD/CHF, USD/JPY, and EUR/USD resulting from heavy-tailed spreads for USD/JPY and EUR/USD returns and heavy-tailed spreads and long-range relations for USD/CHF returns, with GBP/USD, returns showing monofractal nature.

We used the VARFIMA model as a forecasting method by improving the work done for VARMA since VARMA has been very effective in forecasting economic data with exceptional results over related models in multivariate cases (Lutkepohl and Poskitt, 1996). Kapetanios and Gustavo (2014) agree that VARMA methods prefer forecasting medium and big datasets than VAR and AR models, in particular.

In our thesis, we used WTC to demonstrate the relationship and association between exchange rates and investigate the fractal behavior of these time series by MFDFA. We use some exchange rates daily prices: USD/CAD, USD/GBP, USD/CHF, and USD/EUR to obtain better conclusions about this chapter. We aim to add literature to achieve meaningful results for practical use by offering an efficient way to implement wavelet coherence analysis and the VARFIMA forecasting method jointly.

Karatas, C. et al. (2017) and Yılmaz, A. et al. (2017) examined correlations and co-movements of real estate markets through WTC, and these results are used for forecasting in VARMA models. Here, we developed and used MWC for correlations and co-movements of four exchange rates and examined the multifractal behavior of these time series by MFDFA. If a time series illustrates multifractal behavior, there is a long memory. In VARMA, the outcome of this thesis produced better results than before. Compared to the three-time series, VARFIMA works well. For VARFIMA, coherent scales for multiple data series offer required input. If a time series has a long memory, it shows better forecasting results. Section 2 begins with the methods and brief presentation of wavelet analysis, cross wavelet transformation, MF-DFA and VARFIMA. Section 3 discusses the findings of the WTC, MWC, MF-DFA and forecasting the last part of the chapter ends with the observations of the results of the chapter.

1.2. Methodology

1.2.1. Wavelet coherence (WTC)

In this chapter, WTC was used to identify complex associations in the time series of exchange rates. By wavelet coherence, we measured the two-time series’ co-movements. If they are correlated, there are coherence areas represented by red to blue colors in the wavelet coherence figures that illustrate high to low-level coherence for a given period. In casual relationships, phase angle stats give feedback. The arrows analyze the series' co-movement in figures in a time interval; when arrows move right in a given period, they are in phase, so they co-move. There are advantages of wavelet analysis over Fourier transform. In time and frequency, the wavelets have a zero mean. Hence, wavelet analysis can be used to evaluate time series that at several different frequencies contain non-stationary control. The theory of Heisenberg instability stated it is always a tradeoff among frequency and time. By wavelet transform approaches, ambiguity can be reduced.

Wavelet tools invented by Grinsted et al. (2004) are used in this thesis for two-time series, and we have developed this package for four-time series. We choose Morlet Wavelet because it gives a strong balance among frequency and time. Phase relationships of two-time series and four-time series analyzed that are not normally distributed in frequency and time domain. The time series of CWT (Continuous Wavelet Transform) can be excellently decomposed and then restored. For feature extraction purposes, CWT is extremely effective. Two CWTs are used to form the Cross Wavelet Transform (XWT). In frequency-time space, XWT shows the mutual power of two-time series and their relative phase. The causal connections are illuminated by phase interactions among the series.

CWT works on the x(t) sequence like a bandpass filter and is described via twist;

$$W_x(\tau, s) = \frac{1}{\sqrt{s}} \sum_{t=1}^{N} x(t)\varphi^*\left(\frac{t-\tau}{s}\right) \tag{1.1}$$

Here * is complex conjugate, φ is morlet wavelet, the transformation parameter is "τ" and it is time in the transform domain, “s” is the scale parameter which is the frequency in this domain.

Morlet Wavelets, developed by Morlet, Grossman, and Goupillaud (1984), were used in this thesis and described below;

$$\varphi(\eta) = \pi^{-1/4} e^{i\omega_0\eta} e^{-1/2\eta^2} \tag{1.2}$$

here η is time, and ω_0 is frequency chosen 6 because it offers a strong match among frequency and time domain (Grinsted et al., 2004). For various causes, Morlet wavelets are particularly preferred, such as low area of Heisenberg box, size to frequency transformation capability, excellent balance among time and frequency concentration, and quantitative odds.

$W_n^X(s)$, W_n^Y(s); wavelet transforms of X, Y, and their XWT is;

$$\Psi_n^{XY}(s) = W_n^X(s).W_n^{Y*}(s) \tag{1.3}$$

Here, $W_n^{Y*}(s)$ is complex conjugate of $W_n^Y(s)$.

So one can define the wavelet coherence (WTC) as;

$$R_n^2(s) = \frac{|S(\, s^{-1}\Psi_n^{XY}(s)\,)|^2}{S(\, s^{-1}|W_n^X(s)\,|^2).S(\, s^{-1}|(W_n^Y(s)\,|^2)} \tag{1.4}$$

Here S is smoothing operator, and “***s***” is a wavelet scale.

1.2.1.1. Phase

Description of WTC's phase difference is;

$$\varphi_{xy}(u,s) = tan^{-1}\left(\frac{I\{S((s^{-1}\Psi_n^{XY}(u,s)))\}}{R\{S((s^{-1}\Psi_n^{XY}(u,s)))\}}\right) \quad ,\varphi_{xy} \in [-\pi,\pi] \tag{1.5}$$

Here: R and I; real and imaginary pieces of the power spectrum. Phase differences among series tell how they co-move at distinct scales. If the arrows move right, the time series are co-moved, so in phase. If arrows move up (phase difference on $[0,\pi/2]$), second lead first. If arrows move down (phase difference on $[0,-\pi/2]$), then the first leading.

1.2.2. Multiple wavelet coherence (MWC)

MWC is a methodology that behaves as multiple associations and allows identifying the connection of four-time series to each other. MWC is an application of the bivariate wavelet coherence case. The association of significant parameters x_1 and x_2 against other parameters is kept in mind when measuring coherence and phase differences. The squared MWC among x_1 and $x_2, \ldots, x_p$ is defined as (1.6)

$$R^2_{1(2,3,\ldots,p)} = R^2_{1(q)} = 1 - \frac{M^d}{S_{11}M^d_{11}} \tag{1.6}$$

$$S_{ij} = S(W_{xixj})(S_{ij} = S^*_{ji}, S_{ij} = S(|W_{xi}|^2)) \tag{1.7}$$

Here, S_{ij} smoothed XWT spectra.

$$M = \begin{bmatrix} S_{11} & \cdots & S_{1p} \\ \vdots & \ddots & \vdots \\ S_{p1} & \cdots & S_{pp} \end{bmatrix} \tag{1.8}$$

M; p x p matrix of S_{ij}.

M_{ij}^{d} is the cofactor of variable in location (i,j) and written like;

$$M_{ij}^{d} = (-1)^{i+j} \det(M_{i}^{j}) \tag{1.9}$$

Here, M_{i}^{j} is the submatrix obtaining off M via erasing i^{th} row and j^{th} colon and $\det M = M^{d}$

Squared multiple WTC can be shown as;

$$R_{1(q)}^{2} = 1 - \frac{C^{d}}{C_{11}^{d}} \tag{1.10}$$

In our thesis, we use four-time series, so we composed the coherence matrix C, which is 4x4 matrix of all smoothed WTCs $\rho_{ij,}$ and the diagonal of a matrix all is one

$$C = \begin{bmatrix} 1 & \rho_{12} & \rho_{13} & \rho_{14} \\ \rho_{21} & 1 & \rho_{23} & \rho_{24} \\ \rho_{31} & \rho_{32} & 1 & \rho_{34} \\ \rho_{41} & \rho_{42} & \rho_{43} & 1 \end{bmatrix} \tag{1.11}$$

ρ_{ij} is shown as;

$$\rho_{ij} = \frac{S(W_{ij})}{\sqrt{S(|W_{xi}|^{2})S(|W_{xi}|^{2})}} \tag{1.12}$$

The C_{11}^{d} is derived from;

$$C_{11}^{d} = \begin{bmatrix} 1 & \rho_{23} & \rho_{24} \\ \rho_{32} & 1 & \rho_{34} \\ \rho_{42} & \rho_{43} & 1 \end{bmatrix} \tag{1.13}$$

Then if we solve the (1.13);

$$C_{11}^{d} = 1 - \rho_{23}\rho_{32} - \rho_{24}\rho_{42} + \rho_{23}\rho_{32}\rho_{42} + \rho_{24}\rho_{32}\rho_{43} - \rho_{34}\rho_{43} \tag{1.14}$$

$$C_{11}^{d} = 1 - R_{23}^{2} - R_{24}^{2} - R_{34}^{2} + 2R(\rho_{23}\rho_{34}\rho_{24}) \tag{1.15}$$

In equation (1.15), $\rho_{23}\rho_{32}$ stated as R_{23}^{2}

We derived C^{d} on (1.15) as;

$$C^{d} = C_{11}^{d} - \rho_{12}C_{12}^{d} + \rho_{13}C_{13}^{d} + \rho_{14}C_{14}^{d} \tag{1.16}$$

$$\begin{aligned} C^{d} = {} & 1 - R_{12}^{2} - R_{13}^{2} - R_{23}^{2} - R_{14}^{2} - R_{24}^{2} - R_{34}^{2} + \rho_{12}\rho_{23}\rho_{31} \\ & + \rho_{13}\rho_{21}\rho_{32} + \rho_{12}\rho_{24}\rho_{41} + \rho_{23}\rho_{32}\rho_{41} - \rho_{14}\rho_{13}\rho_{24}\rho_{32}\rho_{41} \\ & + \rho_{13}\rho_{24}\rho_{31}\rho_{42} - \rho_{13}\rho_{21}\rho_{34}\rho_{42} + \rho_{23}\rho_{34}\rho_{42} + \rho_{14}\rho_{31}\rho_{43} \\ & - \rho_{12}\rho_{24}\rho_{31}\rho_{43} - \rho_{14}\rho_{21}\rho_{32}\rho_{43} + \rho_{24}\rho_{32}\rho_{43} + \rho_{12}\rho_{21}\rho_{34}\rho_{43} \end{aligned} \tag{1.17}$$

If we write (1.15) and (1.16) to (1.17), we can obtain the detailed squared MWC formula that is used in the mathematical calculations;

$$R_{1(234)}^{2} = 1 - \frac{C^{d}}{C_{11}^{d}} \tag{1.18}$$

We also explained the Eq. (1.17) in terms of our exchange rates (x_1, x_2, x_3, x_4) ;

$$\begin{aligned} C^{d} = {} & 1 - R^{2}(x_1,x_4) - R^{2}(x_4,x_2) + 2[R(x_1,x_2) \cdot R(x_1,x_4)^{*} \cdot R(x_4,x_2)^{*}] \\ & - [R^{2}(x_1,x_2) + R^{2}(x_3,x_4)] + 2[R(x_1,x_3) \cdot R(x_3,x_4) \cdot R(x_1,x_4)^{*}] \\ & + [R^{2}(x_1,x_2) \cdot R^{2}(x_3,x_4)] - 2[R(x_4,x_2) \cdot R(x_1,x_3) \cdot R(x_3,x_4) \cdot R(x_1,x_2)^{*}] \\ & + 2[R(x_4,x_2) \cdot R(x_3,x_4) \cdot R(x_3,x_2)^{*}] - 2[R(x_1,x_4)^{*} \cdot R(x_1,x_2) \cdot R(x_3,x_4) \cdot \\ & R(x_3,x_2)^{*}] - R^{2}(x_1,x_3) - [R^{2}(x_4,x_2) \cdot R^{2}(x_1,x_3)] - 2[R(x_4,x_2) \cdot R(x_1,x_4) \cdot \\ & R(x_3,x_2)^{*} \cdot R(x_1,x_3)^{*}] + 2[R(x_1,x_2) \cdot R(x_3,x_2)^{*} \cdot R(x_1,x_3)^{*}] - R^{2}(x_3,x_2) + \\ & [R^{2}(x_1,x_4) \cdot R^{2}(x_3,x_2)] \end{aligned} \tag{1.19}$$

1.2.3. Fractal Theory and Long Memory

Fractals are bringing order to complexity and elegance to chaos. Many of the earth's natural systems and time series are believed to be identified in fractal form. Fractal structures are self-similar to the region. Basically, we're going to work with a fractal dataset by analyzing exchange rates; USD/CAD, USD/GBP, USD/CHF, USD/EUR.

The features of a fractal are defined by Falconer[1990] shown below:

(a) Classic Euclidean geometric concept wasn't adequate for irregular and complex forms

(b) Fractality has infinite specifics on every scale

(c) İt is a fractal structure of self-similarity. It means that the pieces of the design are like the whole

(d) In many other situations, it could be an easy way of describing it.

In the financial sector, several studies explored the fractal process. The nonlinear features of securities and foreign exchange markets were primarily studied. The fractal characteristics of European and US stock markets were studied by Onali and Goddard (2011) and Robert F. Mulligan (2004). Via adding fractal action, Batten and Ellis (1996) and Gordon R. Richards (2000) validated the exchange rates.

1.2.4. Fractal analysis and MF-DFA

The geometric fractal scale of time series is determined by the Hurst Exponent (H). If X(t) sequence is a fractal, thus X(at) is statistically equal to $a^H X(t)$. There were some approaches for getting H. In this research, we used non-parametric quantitative tools of rescaled range (R/S) methodology.

The R/S method is represented below:

The sequence {Rt} of size N has to be divided by Y (integer) groups of subseries. Subseries of size n of subseries were stated as Iy (y=1, 2, 3,..., Y). The subseries' data are $R_{k,\,y}$ (k=1, 2, 3,...n). The total divergence of the variables from the mean for every component is determined after determining the mean (m_y) of the sub-series

$$X_{k,y} = \sum_{i=1}^{k} \left(R_{i,y} - m_y\right), k = 1,2,3,\dots,n \tag{1.20}$$

The range (R_y);

$$R_i = \max\left(X_{k,y}\right) - \min\left(X_{k,y}\right), k = 1,2,3,\dots,n \tag{1.21}$$

The subseries standard deviation:

$$S_y = \sqrt{\left(\frac{1}{n}\right) \sum_{k=1}^{n} (R_{k,y} - m_y)^2} \tag{1.22}$$

The subseries' R/S mean value:

$$(R/S)_n = \left(\frac{1}{Y}\right) \sum_{y=1}^{Y} \left(R_y - S_y\right) \tag{1.23}$$

The Hurst exponent fundamental concept is:

$$\mathrm{E}(R/S)_n = C * n^H \tag{1.24}$$

Here: C is a constant, H is the Hurst exponent, and n is the length of time periods.

The relationship among the Hurst and D (fractal dimension) is:

$$H = 2 - D \tag{1.25}$$

The Hurst Exponent, H, could also be determined as;

$$H = \frac{\log(R/S)}{\log(N)} \tag{1.26}$$

Here R/S is rescaled range, N is the length of data.

Random walk time series has H=0.5. It is proof of the hypothesis of an efficient market. This is to add that incidents are not related, and the market also has ignored or even missed the influence of previous information. The sequence follows fractional features if H is not equal to 0.5 (i.e., biased random walk).

If 0.5<H, it means there is a continuity of time series, and it is a representation of long memory. The nearest H to 1, the continuity is greater.

In order to define the scaling properties, a multifractal time series needs an unlimited amount of indexes. It is possible to separate multifractals into several sub-sets distinguished by various Hurst exponents. The generalized multifractal dimension denotes the Hurst exponent-characterized fractal dimension of the set.

The purpose of this research is to investigate the fractal behavior of exchange rates, whose numerical characteristics differ through time. We also believe that study of multifractal trends in the exchange rate is used to estimate better forecasting.

We use MFDFA (Multifractal De-Trended Fluctuation Analysis) to examine the fractal behavior of exchange rates.

The method for measuring MFDFA is defined as:

The function of q^{th} order fluctuation is determined by;

$$F_q(n) = \left\{ \frac{1}{N_n} \sum_{s=1}^{N_n} \left[\frac{1}{y} \sum_{y=(s-1)n+1}^{sy} \left[X_y - X_{ys}\right]^2 \right]^{\frac{q}{2}} \right\}^{\frac{1}{q}} \qquad (1.27)$$

Here, the local trend is X_{YS}, q all values except 0. $F_q(n)$ rises by n with respect to the power law of $F_q(n) \sim n^{h(q)}$ if there are long-term correlations.

The slope of the regression of log n with log Fq(n) is the generalized Hurst exponent h(q). H(q) is independent of q for the monofractal dataset, although it is a decreasing function of q for the multifractal data series. The scale of multifractality is computed by $\Delta h = h(q)_{max} - h(q)_{min}$. A larger value of Δh lead to greater variation in the scaling of fluctuations of various size.

1.2.5. Vectorial ARFIMA (VARFIMA) Models

The basic purpose of this research is to show that VARFIMA methods provide more substantial fractal time series prediction outcomes. VARFIMA Process is used as the forecasting tool for our thesis to receive and use the discovered knowledge for extremely delicate output over existing algorithms on interdependency among data series.

In addition, it is simple to prove that by applying wavelet transform, scraping of data with the same frequency would increase the forecasting results because of more strongly correlated time series gotten.

VARFIMA Method analyzes the data in the previous values of interconnected variables in the prediction of chosen coupled time series variables concurrently via building a vector, thus allowing more accurate forecast results.

The data move with equal frequency would cause a decline in the values of the deviation when using strongly correlated and multifractal data in a vectorial model.

The autoregressive fractionally integrated moving average time series (p, d, q) process method, described via ARFIMA (p, d, q), where p is the number of time lags of autoregressive model, d is differencing degree and $d = H - \frac{1}{2}$, and q is the moving-average model's order, by a mean μ, can be described with function terminology as;

$$\alpha(E)(1-E)^d(y_t-\mu)=\beta(E)\varepsilon_t\,,\varepsilon_t\sim i.i.d.(0,\sigma_\varepsilon^2) \qquad (1.28)$$

Here; E is backward-shift operator,

$\alpha(E)=1-a_1E-\cdots-a_pE^p$ and $\beta(E)=1+b_1E+\cdots+b_qE^q$,

Here; $(1-E)^d$ is the operator of fractional differentiation described as,

$$(1-E)^d=\sum_{k=0}^{\infty}\binom{d}{k}(-E)^k=1-dE+\frac{d(d-1)}{2!}E^2-\cdots \qquad (1.29)$$

The function supports the vectorial ARFIMA method of orders p and q as a y_t, m dimensional time series' vector, in which $\alpha_0,\alpha_1,\alpha_2,\dots,\alpha_p$ and $\beta_0,\beta_1,\beta_2,\dots,\beta_q$ matrices of order m*m and ε_t are a vector of disturbance.

$\alpha(z)=1-a_1z-\cdots-a_pz^p$ and $\beta(z)=1+b_1z+\cdots+b_qz^q$ are matrix valued polynomials.

The arbitrary restriction of d to integer values gives rise to ARIMA model. For $d\in(0,0.5)$, the ARFIMA process is said to be displayed long memory, or long-range positive dependence.

1.3. Empirical Outcomes

1.3.1. Data

USD/CAD, USD/GBP, USD/CHF, and USD/EUR daily prices were downloaded from Investing.com. The exchange rates were analyzed for about ten years between 01/01/2009 and 05/12/2019 for WTC and MFDFA methods.

Table 1.

Descriptive Statistics of Exchange Rates

	Mean	Median	Std.Dev	Skewness
USDEUR	0.7683	0.7652	0.01955	0.8090
USDCHF	0.9353	0.9326	0.01974	0.5699
USDGBP	0.6376	0.6374	0.01350	0.3173
USDCAD	1.0115	1.0119	0.0201	0.1512

From Table 1, it can be seen that USDCAD has a standard deviation (0.201); thus, it is a higher oscillation for prices of USDCAD w.r.t. other exchange rates. The positive skewness of zero often means low losses and some excessive gains, which is greater for USDEUR (0.8090) due to its low volatility (Std. Dev: 0.01955). If we look at the correlations among exchange rates in Table 2**,** we obtain a higher correlation between USDCHF and USDEUR (0.8833) w.r.t. others.

Table2.

Correlation Between Exchange Rates

	USDEUR	USDCHF	USDGBP	USDCAD
USDEUR	1	0.8833	0.1732	-0.0912
USDCHF	0.8833	1	0.4730	0.2064
USDGBP	0.1732	0.4730	1	0.6796
USDCAD	-0.0912	0.2064	0.6796	1

1.3.2. Wavelet Coherence (WTC) Results

A picture of frequency on the y-axis and time on the x-axis is brought out by the WTC plot. The low frequencies variables offer greater scale values or periods of co-movement. The bar shows the strength of coherence on the right-hand side. The red color implies greater force, and switching to blue implies less coherence among the terms. The cone of the influence area is shown by the thin fading segment along the edges. That is due to the poor effective outcomes achieved at the edges of the datasets by the wavelet transform. The black line-contoured areas show a 5% significance level toward the noise. At the 5% significance stage, the blue area shows no frequency and time dependency.

In phase, the arrows show the relationship among time series. Arrows moving to the right indicate a positive relationship, and a negative relation is indicated to the left. If the arrow is pointed down, in that time and frequency area, the first series affect the second, and the up-pointing arrows show the first series is affected. Here time is on the vertical axis and frequency in days on the horizontal axis.

1.3.2.1. WTC of USDEUR, USDCHF, USDGBP and USDCAD

In Figure 1, the USDEUR-USDCHF plot tells two-time series co-moved in some times and frequencies, and a highest (shown in black circles) between 16/11/2011(day. 750) and 16/08/2017 (day.2250) after the Spain and Italy debt crisis(Sept. 2011) and around Brexit referendum of Britain form EU(23.June 2016) along with the 8-64 day cycles. That is, 1 to 8-week cycles of the USDEUR exchange rate changes and USDCHF exchange rate changes move together. In coherent areas, right moved arrows imply they are in phase, and arrows moved down represent USDEUR leads USDCHF.

Figure 1

WTC of USDEUR-USDCHF. Horizontal line numbers show the dates 500(01/12/2010), 1000 (31/10/2012), 1500 (01/10/2014), 2000 (31/08/2016), and 2500 (01/08/2018).

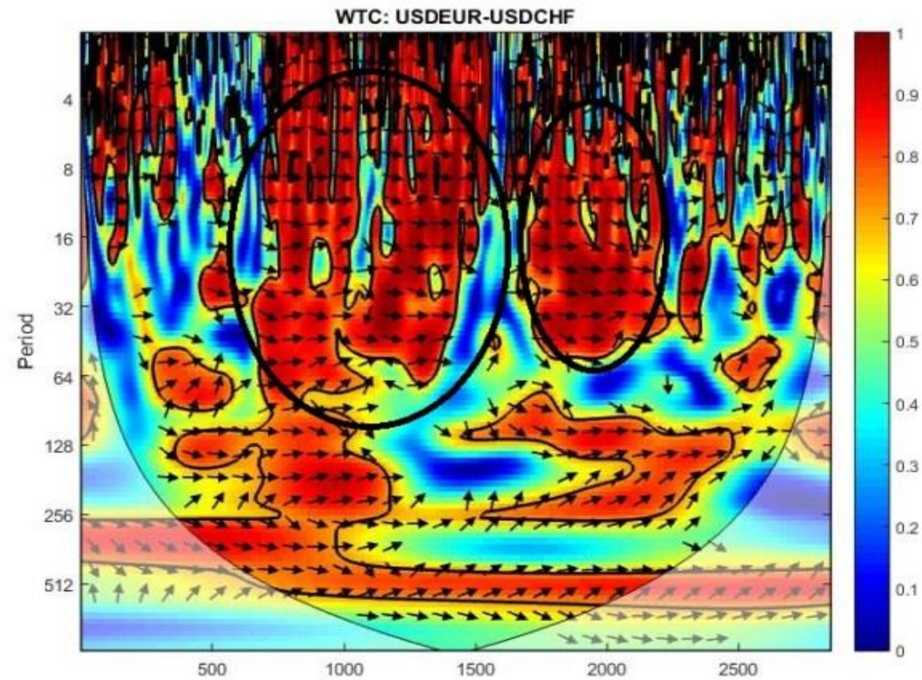

Figure 2

WTC of USDEUR-USDGBP. Horizontal line numbers show the dates

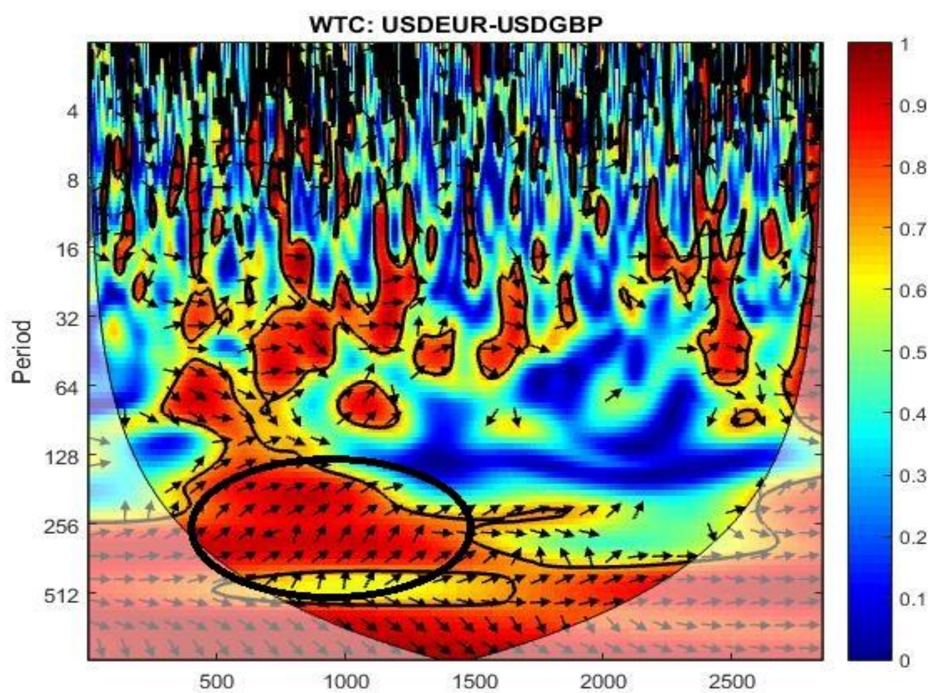

The WTC plot in Figure 2 shows coherence areas in different frequencies almost in the long run. The highest coherent area (shown in black circle) is particularly at 128-512 day cycles between 01/12/2010(day 500) which is after the Irish aid package (30 Nov. 2010) to 01/10/2014(day 1500). The direction of the arrows to the right holds a positive correlation among the time series. These findings and the upward arrows conclude that USDGBP exchange rate movements affect the USDEUR exchange rate changes.

Figure 3

WTC of USDEUR-USDCAD. Horizontal line numbers show the dates

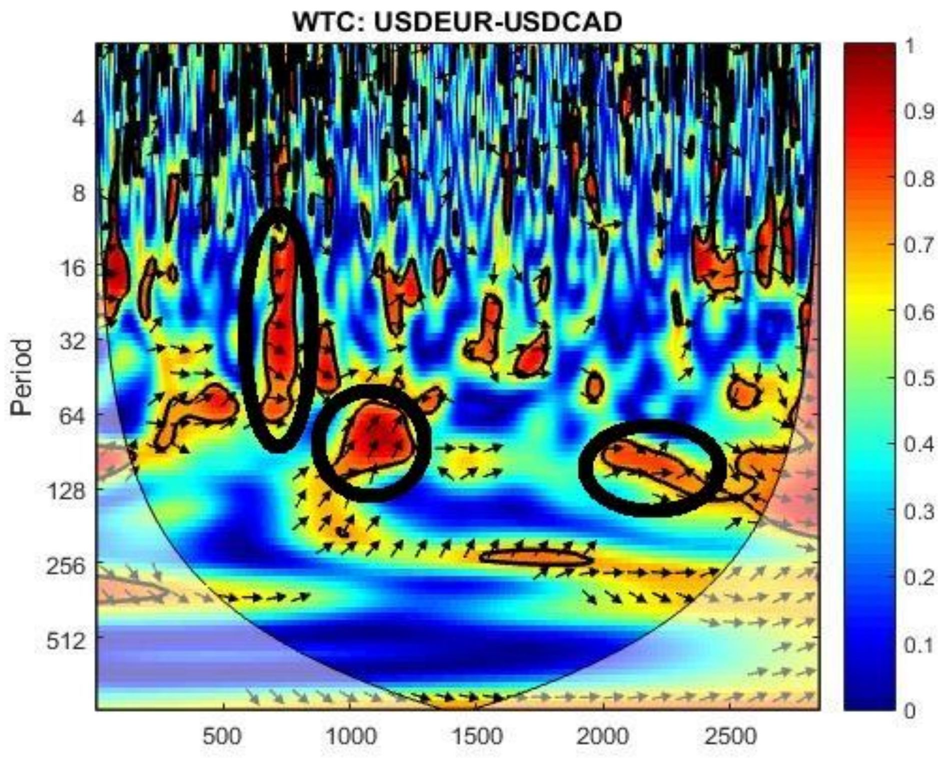

Next, we turn to co-movement between exchange rates USDEUR and USDCAD. As seen in Figure 3**,** specific coherent areas (shown in black circles), especially at days cycles 16-64 between 24/04/2011 (day.600) around Portugal aid package(16 May.2011) to 16/11/2011(day. 750) and also start around 27.06.2012(day. 910) after Spain debt cut (20 June 2012) and around circle 22.06.2016(day. 1950) which is after the Referendum on the separation of Britain from the EU on 23 June 2016. In coherent areas, arrows are pointed to the right. So, time series are positively correlated there.

The co-movement of USDEUR and USDCHF is more than others since the red areas in Figure 1 are higher than other figures, which is supported by the conclusion of a high correlation between them in Table 2 (0.8833).

1.3.3. Multiple Wavelet Coherence (MWC) Results

After explaining the MWC method for four-variable scenarios, we based on our thesis data. In that thesis, four exchange rates were considered since we wanted to explain the effect among USDEUR, USDCHF, USDGBP, and USDCAD. By the MWC formula, we find the MWC of the exchange rates given in Figure 4**.** These figures display the regions (stated time intervals) of correlation among the time series.

MWC(USDEUR-USDCHF-USDGBP-USDCAD) plot in Figure 4 shows that four-time series are correlated and have the same highest coherent regions (Same Black Circle areas on four plot) at day cycles 32-256 between 16.11.2011(day. 750) to 16.10.2013(day. 1250), especially on the EU debt crisis. We use these common coherent times for the forecasting analysis on VARFIMA. You can see from Figure 4a has more coherent areas (red areas) than other figures. So, USDEUR dominated the other exchange rates, and from Figure 4d**,** USDCAD has less impact on others.

Figure 4

MWC of (USDEUR-USDCHF-USDGBP-USDCAD. Horizontal line numbers show the dates

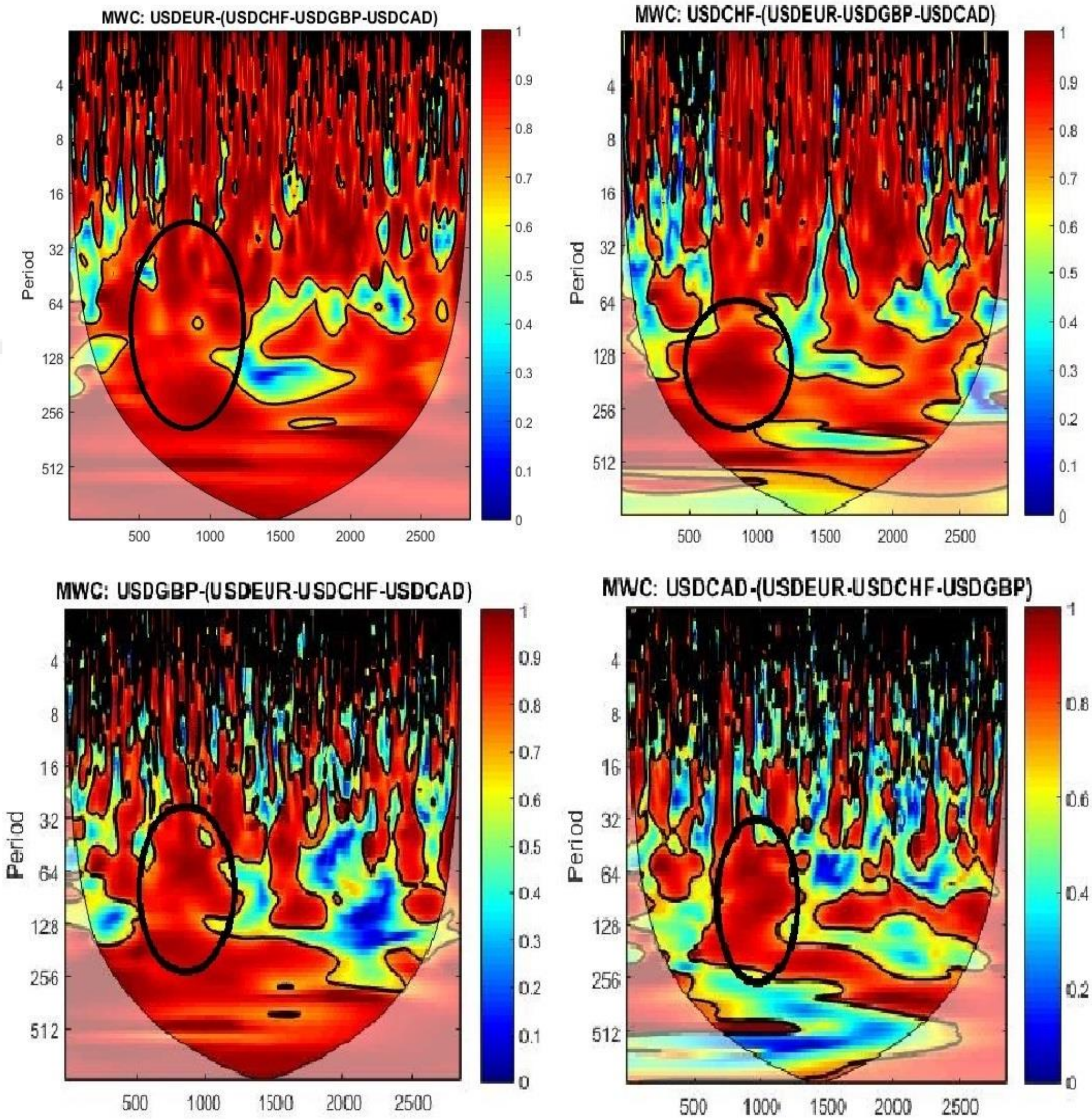

1.3.4. MFDFA and Long Memory Tests Results

We use the MFDFA package in the Matlab session constructed by F.Ihlen (2012) to obtain the figures and MFDFA results. In this package, Matlab codes are used for detecting long memory and multifractality in time series.

We calculate the Hurst exponents for each exchange rate by Matlab codes 5 and find that H is an increasing function indicating multifractal behavior of price changes (Figure 5). The highest Hurst exponent value is 0.53(USDEUR), suggesting that USDEUR has more apparent small fluctuations than other exchange rates. The larger Hurst exponent, H, is seen as more slove-evolving variations (more persistent structure) in USDEUR compared with different exchange rates.

We quantify the generalized Hurst exponents for each exchange rate and find that h(q) is a decreasing function of q at all times, suggesting a multifractal structure of rates volatility (Figure 6A), which implies that these data sets, multifractal methods are sufficient. The degree of multifractality (Δh) is also seen in Table 3 and Figure 6C. It defines how far multifractality is from the system. The bigger the Δh, the larger the multifractality it has.

In Table 3**,** we see the max, min, and different values of q-generalized Hurst exponents for four exchange rates. In the USDGBP, with its rate of $\Delta h = 0.4439$, we note the largest multifractality level. For USDEUR, another outstanding Δh value suggesting a high multifractality degree is observed as Δh=0.3233, respectively. The lowest value of $\Delta h = 0.30$ in USDCAD has the lowest multifractality degree.

Notice that the USDCAD and USDCHF have apparent slow fluctuations, but USDGBP and USDEUR are more compared to others (Figure 5).

USDGBP has max width compared to others (Figure 6C). This suggests that USDGBP shows much multifractal behavior compared to others.

With the calculation, the degree of multifractality of USDCAD is the smallest, and USDGBP is the largest. Outcomes suggest that a high level of multifractality, which reflects a more localized price fluctuation or persistent feature than other exchange rates, is regarded by USDGBP.

Table3.

q-generalized Hurst Exponents for the four time series

Data	Δh	h_{max}	h_{min}
USDEUR	0.3233	0.718	0.3947
USDCHF	0.3192	0.6034	0.2842
USDGBP	0.4439	0.7079	0.264
USDCAD	0.3007	0.6163	0.3156

Figure 6A Hurst exponent with q-order Hq Figure 6C The arrow shows the difference among the highest and the lowest hq, which is named the multifractal spectrum width.

Figure 7A Hurst exponents Ht (lower panel) and exchange rates (upper panel). Figure 7B Hurst exponents Ht’ probability distribution Ph, predicted as histograms. Figure 7C The Dh multifractal spectrum is calculated through the Ph distribution with the same data set. According to Figure 7B, 7C, Spectrum Dh and distribution Ph has a greater width of USDGBP relative to all other exchange rates which means it shows the most multifractal behaviour

The multifractal time series shows small fluctuations (persistent characteristic) and have a long memory, which we show in this section, giving us better forecast results.

Figure 5.

Hurst Exponents of USDEUR-USDCHF-USDGBP-USDCAD.

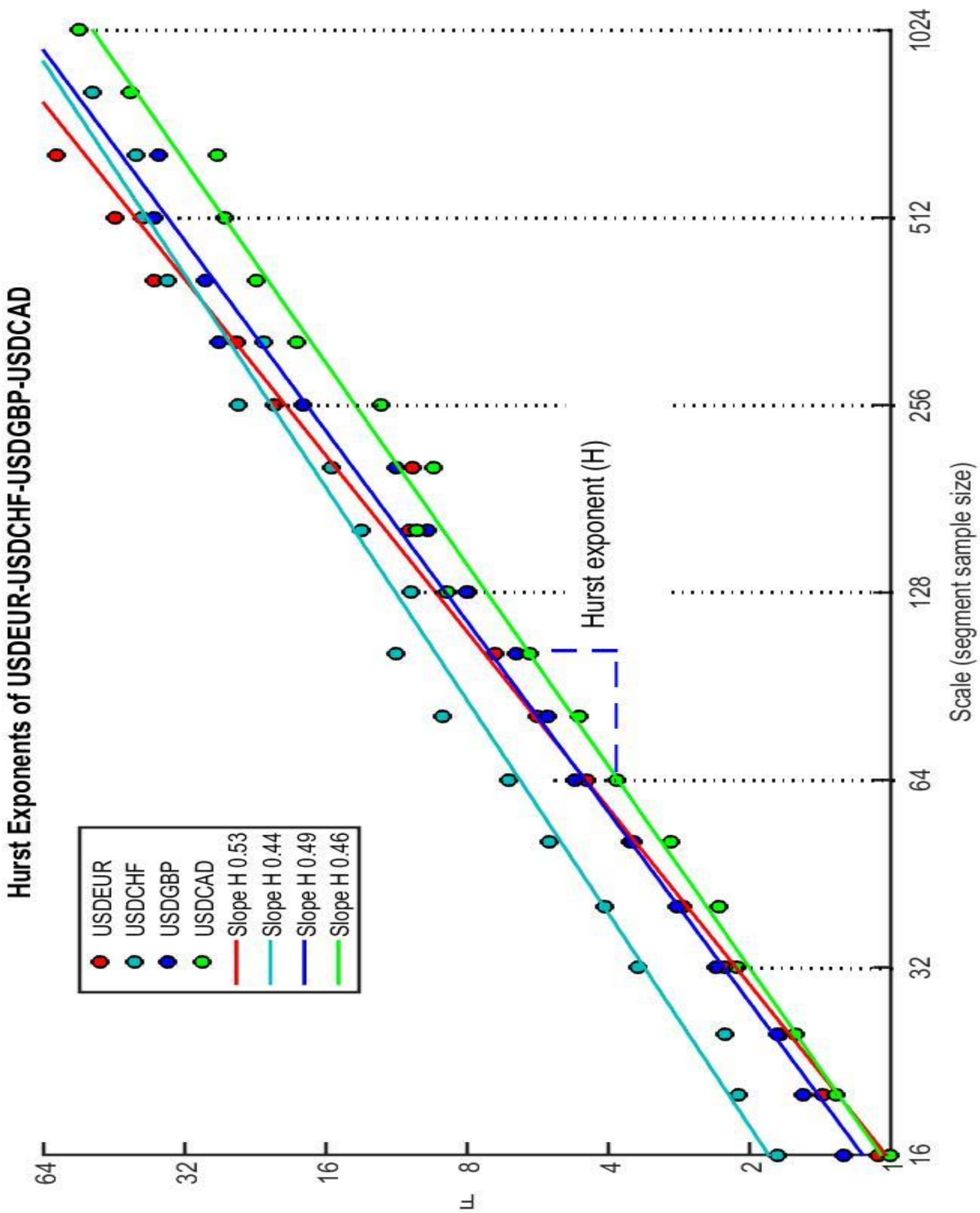

Figure 6.

Multifractal representations of multifractal spectrum for USDEUR (blue traces), USDCHF (red traces), USDGBP (turquoise traces), and USDCAD (pink traces) time series.

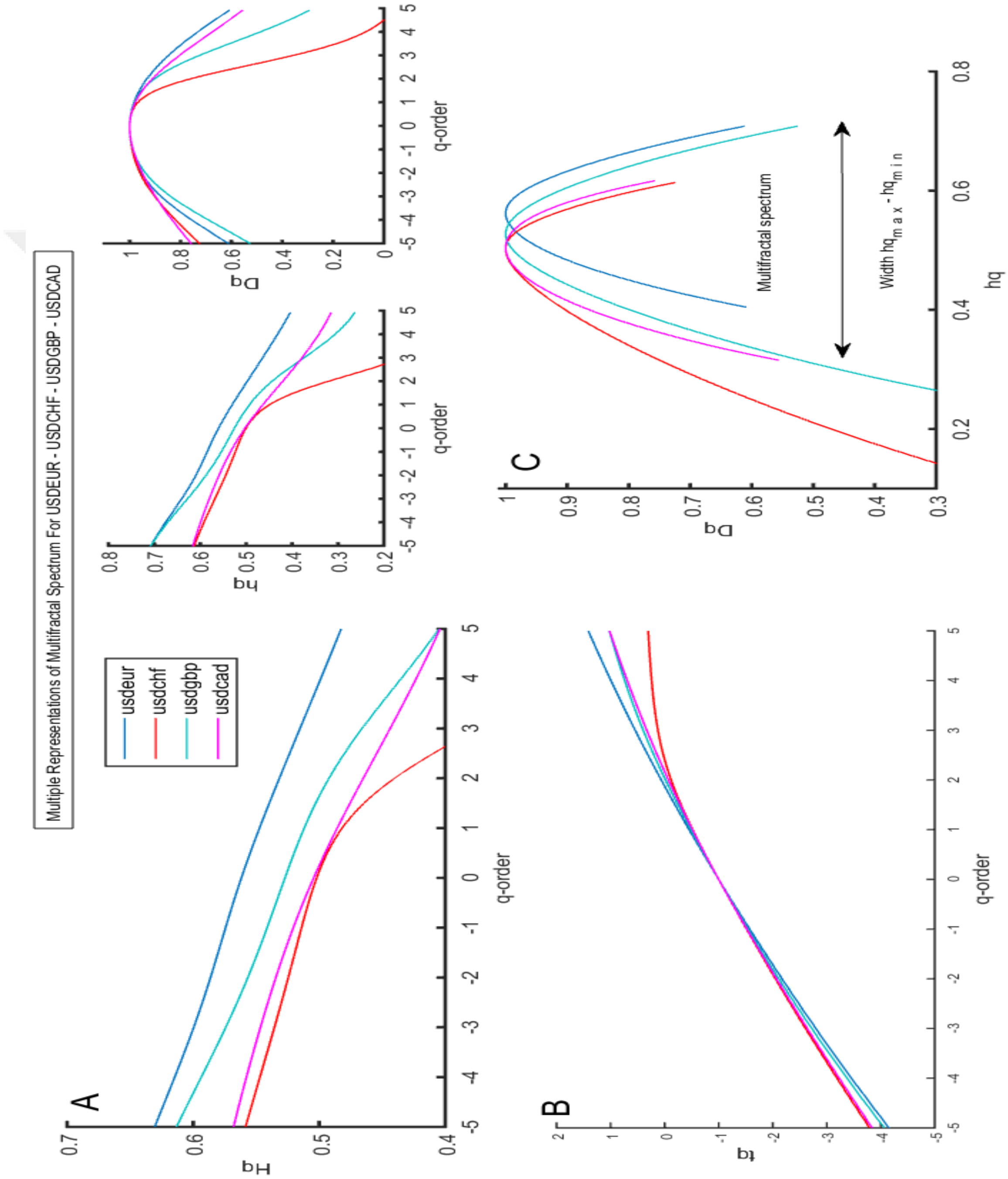

Figure 7.

Multifractal Spectrum of Time Series of USDEUR (blue traces), USDCHF (red traces), USDGBP (green traces), and USDCAD (turquoise traces) time series.

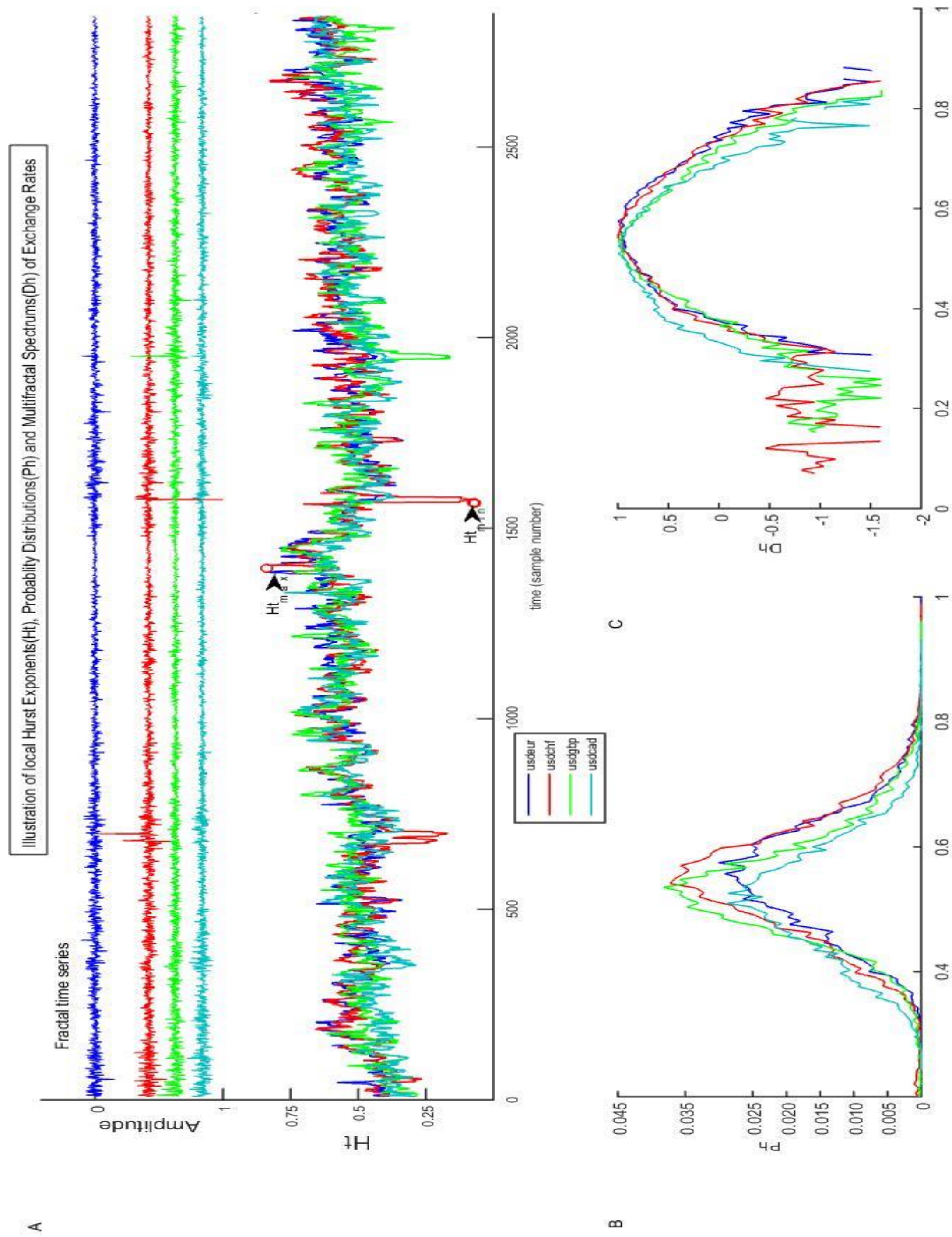

1.3.5. VARFIMA Models, Forecast Results

According to the Table 3, the max Hurst exponent is H=0.71 and since differencing order can be calculated by $= H - \frac{1}{2}$, we take value of d=0.2, p=2 and q=1 fit the data more precisely.

In VARFIMA(2,0.2,1), we use coherent regions (represent time intervals in black circles) in MWC of USDEUR-USDCHF-USDGBP-USDCAD (Figure 4a,b,c,d) and long memory tests, and MFDFA results are used in forecasting since the data which have higher co-movement, long memory, and show fractal behaviour acting via equivalent frequency may cause to a decline in the variance.

Please note that the examination period is between Nov.16, .2011, and Oct.16, .2013, where the co-movement is greater in four-time series about the multiple wavelet coherence analysis. We tested 30 days forecast for the upper bands (UB) and lower bands (LB) via 95% confidence interval.

In Figure 8, the real value of USDEUR is represented in purple, and the forecast is red color. In this scenario, the VARFIMA forecast for USDEUR for the most coherent region found by the MWC from Nov.16.2011 to Oct.16.2013 accurately follows the actual price line. The interval of the upper and lower bound of VARFIMA is narrower than ARMA.

In Figure 9, the real value of USDCHF is represented in purple, and the forecast is red color. Here, for USDCHF, the VARFIMA forecast for the highest coherent region founded by MWC from Nov.16, .2011 to Oct.16, .2013, cannot pursue the actual price line excellently. The confidence interval for VARFIMA is narrower than ARMA.

Figure 8

30 days Forecasting of USDEUR

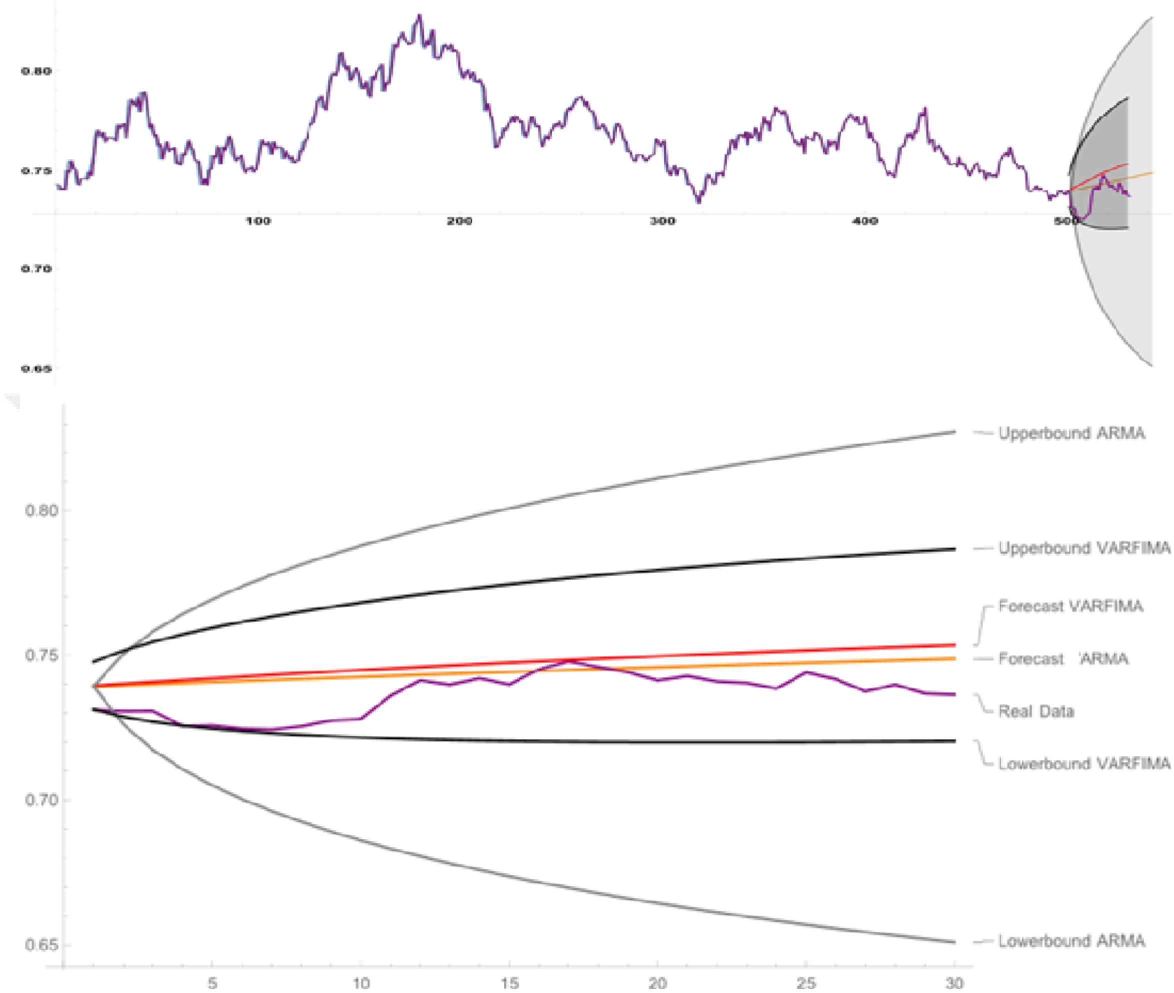

In Figure 10, the real value of USDGBP is represented again in purple, and the forecast is red in color. In this case, for USDGBP, the VARFIMA forecast for the highest coherent region, which was founded by MWC from Nov.16, .2011 to Oct.16, .2013, performed exceptionally well to follow the real price line.

In Figure 11, the real value of USDCAD is represented in purple, and the forecast is red in color. In this case, for USDCAD, the VARFIMA forecast for the highest coherent area founded by MWC from Nov.16 .2011 to Oct.16, .2013, performed the worst to follow the real price line with respect to other exchange rates.

Figure 9

30 days Forecasting of USDCHF

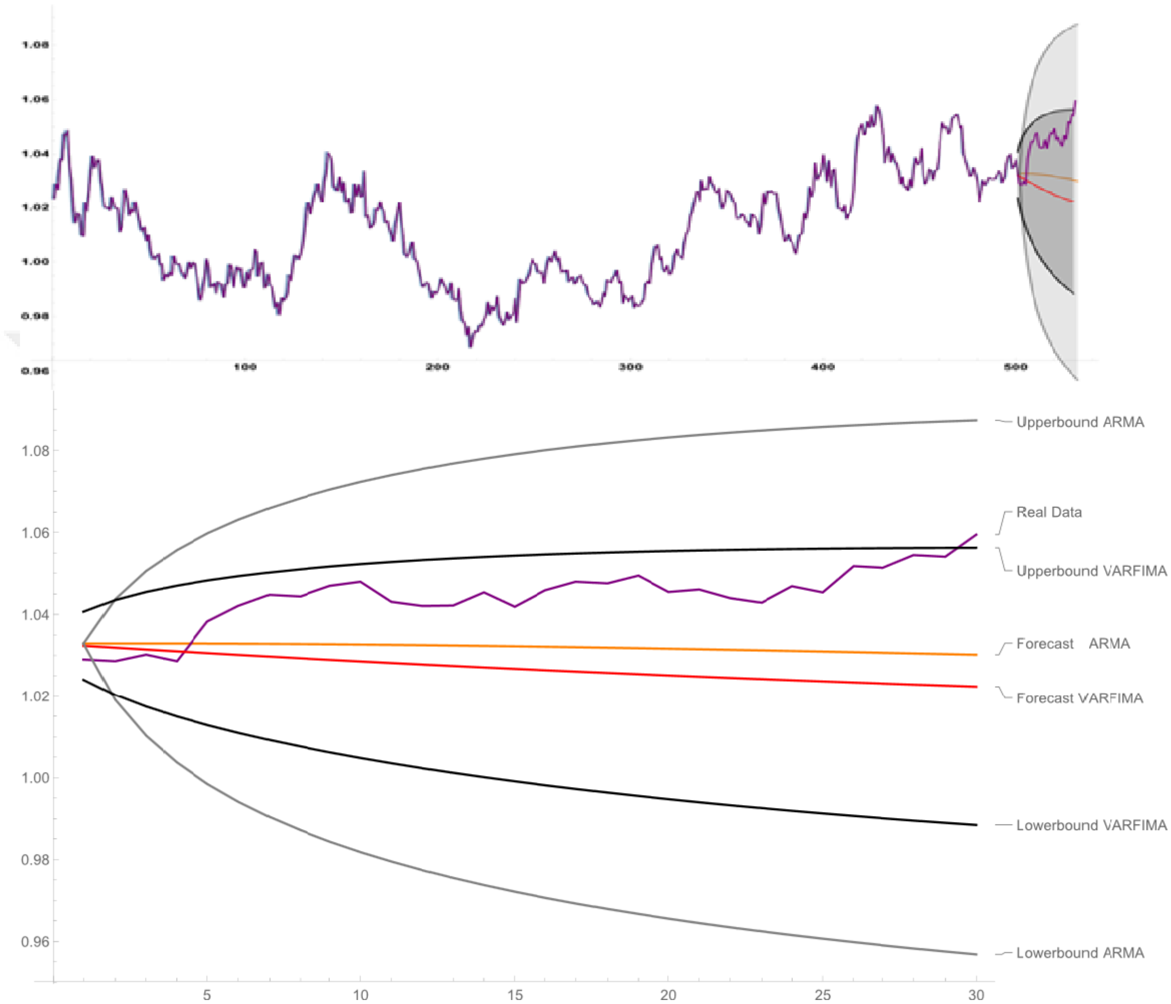

In the case of VARFIMA, 95% confidence intervals within a small area relative to ARMA. We stated that USDGBP works slightly better than the other exchange rates. We match the real data with the expected data by RMS (Root Mean Square) measurement in Table 4, which indicates RMS precision of forecast outcomes because the value of RMS of USDGBP 0.009914 is the lowest. These results promote our theory that if the time series has the highest multifractal degree, it has the most successful forecasting results for the time interval in which four-time series have the highest co-movement.

Figure 10

30 days Forecasting of USDGBP

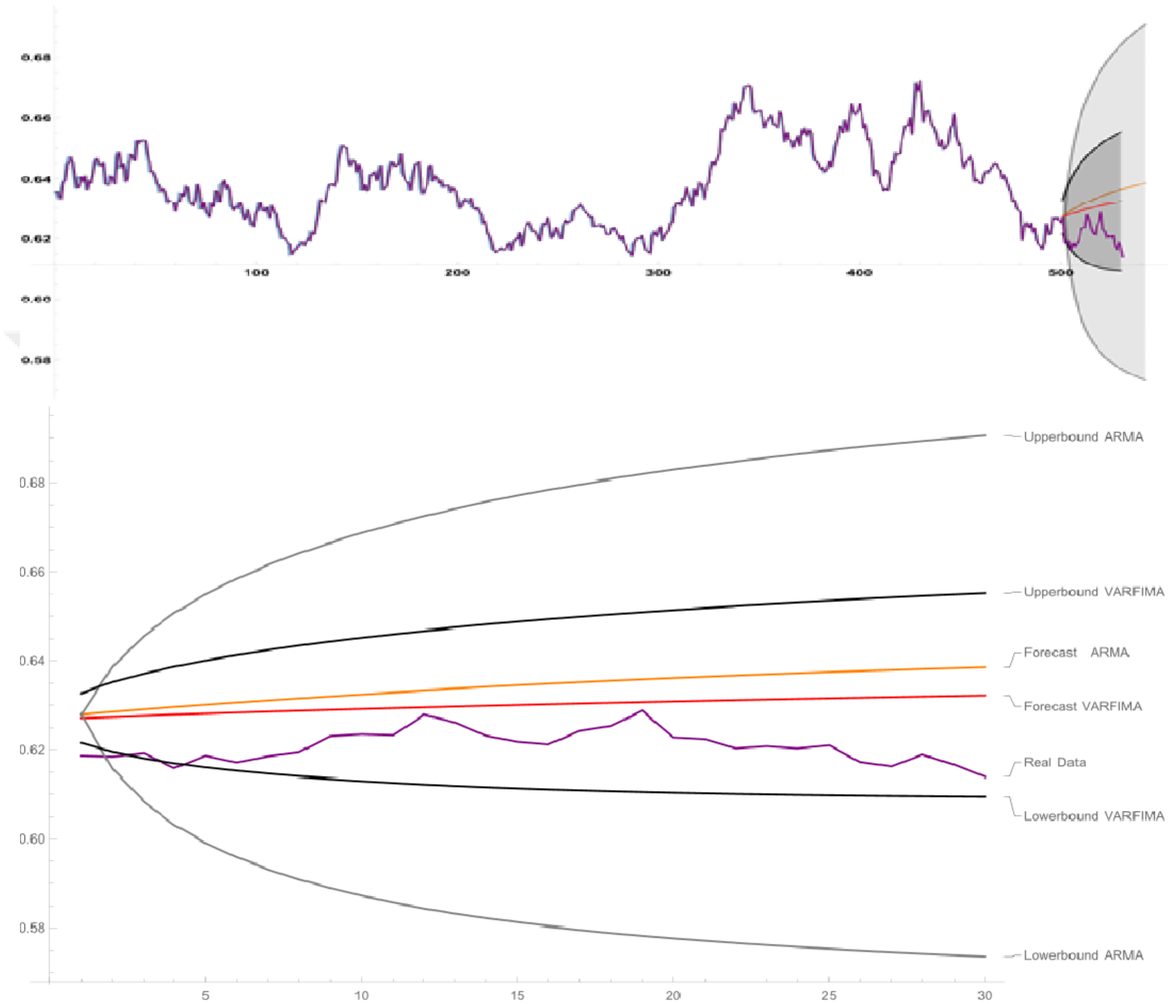

Table 4.

Root Mean Square (Forecast Data – Real Data) Result

	RMS value		RMS value
USDEUR	0.0119001	USDGBP	0.0099143
USDCHF	0.0180562	USDCAD	0.0200924

As seen in the graphs, the model's forecasting accuracy is greatly improved via the VARFIMA method, and on the initial days of the prediction, the model shows considerable accuracy. The USDGBP has better and USDCAD worse forecast result compared to others, and the forecasting precision of the VARFIMA model have a high narrow range compared to ARMA.

Figure 11

30 days Forecasting of USDCAD

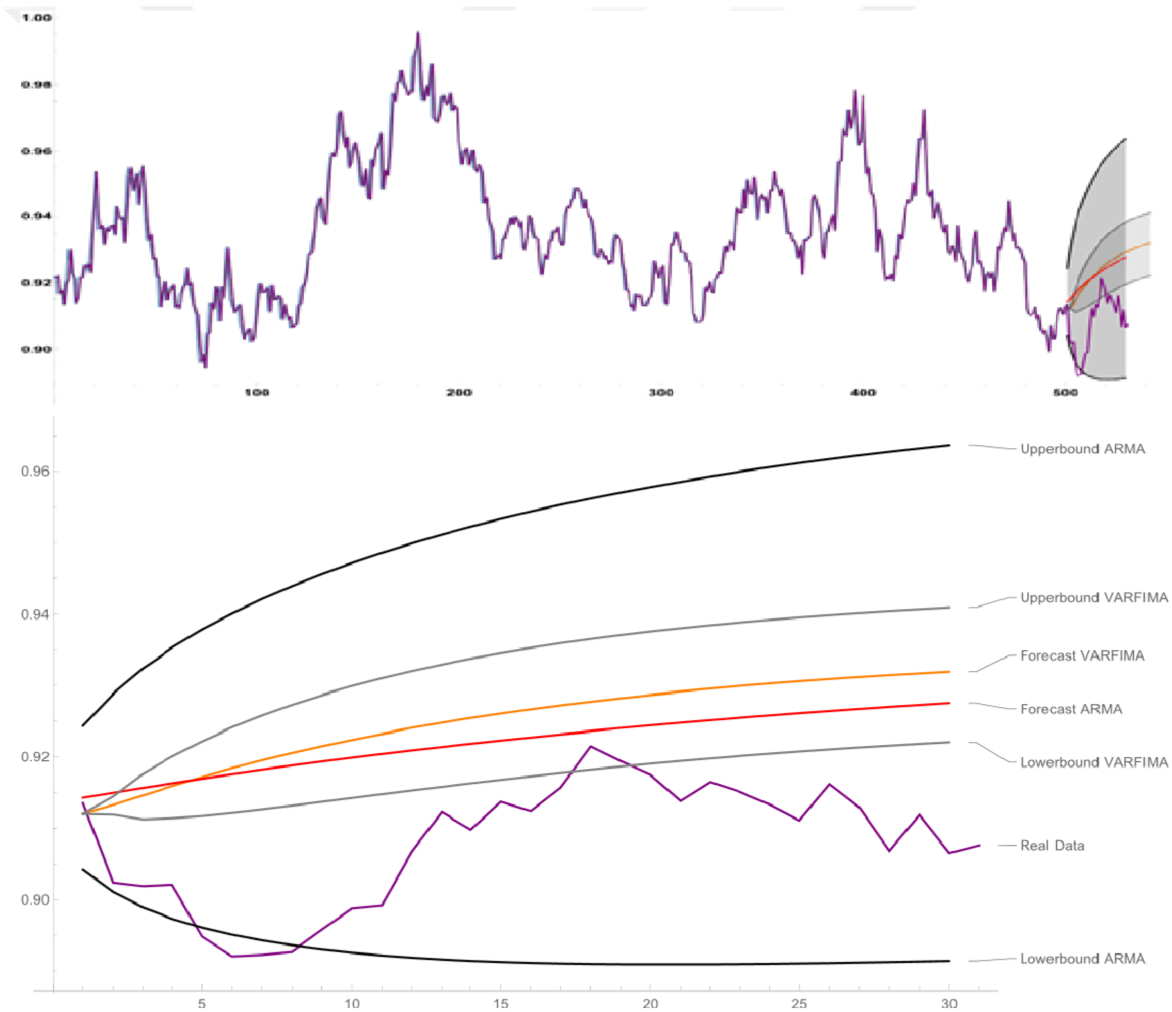

1.4. Conclusion

In this chapter, we gained WTC results and improved and applied MWC of exchange rate time series, USDEUR, USDCHF, USDGBP, and USDCAD. We calculated the time scales and time periods where co-movement is high. We observed that USDEUR and USDCHF showed the highest and USDCAD lowest correlation with other rates at various frequencies and time intervals.

The multifractal time series shows small fluctuations (persistent characteristic) and has a long memory, shown in section 3, giving us better forecast results. Our empirical results show that USDGBP shows higher persistent characteristics. USDCAD has the lowest degree of multifractality, and USDGBP has the highest. The weaker price response to demand that implies reduced rates of efficiency causes a greater degree of price aggregation.

After WTC analysis in forecasting, identified times (correlation areas) are used. All those reported interconnections and dependencies formed the basis for applying the forecast for VARFIMA. Forecasting analysis on VARFIMA, prediction of USDGBP performed the best, and also the value of RMS of USDGBP 0.009914 is the lowest. These results promote our theory since it has a higher multifractal degree and long memory.

In summary, we revealed a correlation among four exchange rates in the frequency and time domain, showed maximum coherence areas, and stated their fractal behavior through the MFDFA model. In addition, for coherent periods, we have established the VARFIMA model. Forecasting focused on VARFIMA models shows smaller errors than the forecast produced from bivariate modeled data set since, in contrast to individual models, multifractality and coherent scales for four-time series offer the ambitioned information for VARFIMA.

CHAPTER 2 WAVELET TRANSFORM GUIDED TRANSFER ENTROPY METHOD FOR NONLINEAR TIME SERIES

Summary

Causality and co-movement between time series have been important studies in the literature for years. The direction of causality and the measurement of information flow continue to be topics for researchers. In this chapter, we acted on this framework. We analyzed the causal relations and co-movement between different exchange rates by transfer entropy (TE) and wavelet coherence (WTC). Transfer entropy, an evaluation for information flows, stated a straight path to examine the relationship between exchange rates also capturing cause and effect relations and in WTC analysis the co-movement between exchange rates can be found and coherent zones may be detected by this method. Fixed Bins and Kernel Density Estimation methods were used for this thesis for TE and for the coherent areas KDE method was used to compare WTC and TE results. In this chapter three different results are obtained: 1) USDGBP is on the leading side, 2) USDCAD dominates other exchange rates on coherent periods and, 3) KDE method could lead to better results. The main conclusion of this chapter, TE through WTC analysis shows, phase angle leading direction change obtained with WTC explains TE sign change. This result indicates both methods give correct output in coherent time zones and financial crisis times like the COVID period which we have faced for two years, for this reason, the results also obtained for the COVID period that shows USDEUR dominated other exchange rates. We interpret this result as the investors adjusting their portfolio positions for exchange rates in financial crisis periods.

2.1. Introduction and Literature Review

The price of a country's currency in terms of foreign currency is the exchange rate, and it is one of the biggest indicators of international trade interaction. For this reason, it has a lot of information about economic conditions and future outlook. For information flow and co-movements between exchange rates, we considered the daily values of currencies. A change in one currency value impacts others after the shocks that happen through financial crisis times. We aim to demonstrate the quantitative methods for connection and innovation of exchange rates, show a correlation among them by WTC and information flows with TE.

There are several methods as a measure of the information flows between time series. The most popular technique is Granger causality (1969) used to explain causal relations between time series. Transfer entropy is a non-linear extension of Granger causality (2009). Transfer entropy proposed by Schreiber (2000), detects the bidirectional information flow between two-time series and information quantity. It is derived from Shannon entropy (1948). If we compared with the mutual information, TE takes the dynamics of information transfer into account and the direction of flow more explicitly. TE has been applied in a lot of areas. Ver Steeg (2012) used this method for social media. Lee et al. (2012) detect the direction coupling change in biomedical time series. Sumioka et al. (2007) used TE on physiological time series. In the area of finance, Yao and Li (2020) investigated information flow among economic policy uncertainty (EPU), stock market and investor sentiment by effective TE which was proposed by Sensoy et al. (2014) explored the information flow between stock markets and exchange rate. Teng and Shang (2017) extended the TE coefficient for quantifying the level of information flow between financial time series. He and Shang (2017) compared the TE methods for financial time series. Mohaghegh et al. (2021) investigated the financial crisis of the Iranian stock exchange using the TE method and compared it with the Dow Jones financial market and Park et al. (2021) studied information flows among financial assets and bitcoin prices.

$TE_{X->Y}$ is the measure of information reduced in future values of Y by knowing the past values of X given past values of Y.

WTC is a method to detect co-movement among time series. Torrence and Compo (1998) defined coherence and cross-wavelet spectra concentrated on atmospheric time series. WTC and cross wavelet transformation methods for two-time series, concentrating on wavelet analysis presented by Grinsted et al. (2004). The use of phase angle statistics was demonstrated in their research to analyze reliance on causal relationships. Tiwari (2012) investigated the connections between interest rates and prices of shares in the Indian economy and inflation, industrial production, and price of oil in the German economy using a cross-wavelet approach. Karatas, C. and Unal, G. (2021) examined co-movements of exchange rates through WTC and their fractal behavior.

In recent years, a lot of studies examining the relationship of time series with each other have been applied in the academic literature. Most of the research was focused on understanding the cause-and-effect relationship between the series. Especially in periods of the financial crisis, besides this cause-effect relationship, the information flow and direction between the series gains importance. As a result of this necessity, in this thesis, we determined the coherence times when the exchange rates moved together by using WTC, and then we investigated the direction of the net information flow in this period by using the TE method and made nonlinear and non-stationary experiments of exchange rate and we named this analysis as Wavelet Transform Guided Transfer Entropy Method (WTGTEM). This is the first study using both WTC and TE.

WTGTEM is a nonlinear and non-stationary generalization of the continuous wavelet transform causality method which was proposed by Olayeni (2016) and as distinct from this method, TE through the WTC method shows, phase angle leading direction change obtained with WTC explain TE sign change. In this methodology, the bidirectional causality and coherence zones between time series in the time-frequency domain are detected by WTC and guided by this analysis the information quantity transferred and the bidirectional information flow between time series measured by TE. Unlike granger causality, TE detects the quantitative direction of information flow and asymmetric qualitative information transfer. WTEGTM allows us to capture the change in the causality and direction of net information flow between the two non-linear and non-stationary time series simultaneously, especially in financial distress periods.

Section 2 starts with Wavelet Transform Guided Transfer Entropy Method (WTGTEM). Section 4 discusses the outputs of WTC and TE and in conclusion, we interpret the results, gains of this chapter.

2.2. Methodology

2.2.1. Wavelet Transform Guided Transfer Entropy Method (WTGTEM)

In this chapter, we proposed Wavelet Transform Guided Transfer Entropy Method (WTGTEM) and in the component of this analysis, first, we determined the coherence zones when the exchange rates moved together and their cause and effect relation through

WTC, and then we investigated the direction of the net information flow in this period by using the TE method.

2.2.2. A Summary for Wavelet Coherence (WTC)

Wavelet coherence indicates the co-movement of two data sets. If they move together, there are coherent zones as in WTC plots that are shown as blue to red colors, indicating low to high degree coherence for a specific timeframe.

Grinsted et al. (2004) invented wavelet tools that were used in this thesis. We choose Morlet Wavelet because it gives a strong balance among time and frequency. The Cross Wavelet Transform (XWT) is created by combining two CWTs (Continuous Wavelet Transforms). XWT displays the mutual strength and relative phase of time series in time-frequency space. The phase difference between this series explains the causal relations. CWT is better at observing the determination of signal frequencies over time and comparing the spectra to those of other signals and a bandpass filter that operates on the x(t) series.

CWT is defined as;

$$W_x(\tau, s) = \frac{1}{\sqrt{s}} \sum_{t=1}^{N} x(t) \varphi^* \left(\frac{t - \tau}{s} \right) \tag{2.1}$$

Morlet Wavelet described below;

$$\varphi(\eta) = \pi^{-\frac{1}{4}} e^{i\omega_0 \eta} e^{-\frac{1}{2}\eta^2} \tag{2.2}$$

Here time is η and frequency is ω_0, which is 6 since it provides a good fit between time and frequency domain.

$W_n^X(s)$, W_n^Y(s); X, Y's wavelet transforms and XWT is;

$$\Psi_n^{XY}(s) = W_n^X(s). W_n^{Y*}(s) \tag{2.3}$$

Complex conjugate of W_n^Y(s) is W_n^{Y*}(s)

Wavelet coherence (WTC) formed as;

$$R_n^2(s) = \frac{|S(\, s^{-1}\Psi_n^{XY}(s)\,)|^2}{S(\, s^{-1}|W_n^X(s)\,|^2).S(\, s^{-1}|(W_n^Y(s)\,|^2)} \tag{2.4}$$

Smoothing operator is “S”.

2.2.2.1. *Phase*

Description of WTC’ phase angle is;

$$\varphi_{xy}(u,s) = tan^{-1}\left(\frac{I\{S((s^{-1}\Psi_n^{XY}(u,s)))\}}{R\{S((s^{-1}\Psi_n^{XY}(u,s)))\}}\right), \varphi_{xy}\epsilon[-\pi,\pi] \tag{2.5}$$

Here: I and R; complex and reel piece of the power spectrum. The co-movement between series at different scales can be detected by phase angles. If they are co-moved and in phase, the arrows move right. If first lead second, arrows act down (phase angle on [0,$-\pi/2$]) and reverse relation when they act up (phase angle on [0,$\pi/2$]).

We applied wavelet transform to time series as Olayeni (2016) to show co-movement and coherence periods between them but after that instead of the granger causality test, we used the TE method to discuss asymmetric cause and effect relation and information flow between time series.

2.2.3. Transfer Entropy (TE)

Shannon published ‘‘Mathematical theory of communication’’ in 1948, it was the first study of the Information theory. Probability theory is used for the analysis of information transfer in information theory. It has been utilized in the disciplines of economics, sociology, statistics, biology, etc. after decades of development. The classical information theory is Shannon's information theory. Shannon's information theory defines information as the reduction of uncertainty. As a result, we may evaluate information by measuring the decrease in uncertainty.

Shannon entropy is defined as follows:

$$H(X) = H(p_1, p_2, \dots, p_k) = \sum_{k=1}^{K} p_k l(x_k) = \sum_{k} p_k log \frac{1}{P(x_k)} = -\sum_{k} p_k log P(x_k) \quad (2.6)$$

$P(x_k)$ denote the probability of x_k.

Mutual information describes the relation between two data sets, it is information of one variable that has information about the other. Consider $p(x, y)$ is the joint distribution of (X, Y), $p(x), p(y)$ are marginal distributions, so, the relative entropy of product distribution $p(x)p(y)$ and mutual information is $MI(X; Y)$.

$$H(X, Y) = H(X) + H(Y|X) = H(Y) + H(X|Y)$$

$$MI(X; Y) = H(X) - H(X|Y) = H(X) + H(Y) - H(X, Y)$$

$$= \sum_{x} p(x) log \frac{1}{p(x)} + \sum_{y} p(y) log \frac{1}{p(y)} - \sum_{x,y} p(x, y) log \frac{1}{p(x, y)} \quad (2.7)$$

$$= \sum_{x} \sum_{y} p(x, y) log \frac{p(x, y)}{p(x)p(y)}$$

Because of the symmetry of the outcomes, with mutual information, information exchange dynamics is not available and we cannot identify relation among causative and passive ones. TE solved this problem. TE can efficiently separate repulsive elements from responsive elements and discover asymmetry in subsystem interactions. The TE describes the amount of information flow from one variable to another.

The definition of TE is;

$$T_{Y\to X} = H(X_{n+1}|X_n) - H(X_{n+1}|X_n\ ,\ \ Y_n)$$

$$T_{Y\to X} = \left[-\sum p(x_{n+1}, x_n, y_n)\log(p(x_{n+1}|x_n))\right] - \left[-\sum p(x_{n+1}, x_n, y_n)\log\left(p(x_{n+1}|x_n, y_n)\right)\right]$$

$$= \sum p(x_{n+1}, x_n, y_n)\log\frac{p(x_{n+1}|x_n, y_n)}{p(x_{n+1}|x_n)} \qquad (2.8)$$

$$= \sum p(x_{n+1}, x_n, y_n)\log\frac{p(x_{n+1}, x_n, y_n)p(x_n)}{p(x_{n+1}, x_n)p(x_n, y_n)}$$

and the opposite direction of TE is

$$T_{X\to Y} = \sum p(y_{n+1}, x_n, y_n)\log\frac{p(y_{n+1}, x_n, y_n)p(y_n)}{p(y_{n+1}, y_n)p(x_n, y_n)} \qquad (2.9)$$

If the net information flow $T_{X\to Y} - T_{Y\to X} > 0$, it means the information flow from X to Y. Direction is the advantage of TE. We can deduce that bidirectional information flow is asymmetric according to the TE formula. We could separate the active and passive factors because of asymmetry.

In this chapter, we use two different methods to estimate TE which are Fixed Bining and Kernel Density Estimation (KDE). We used the Matlab toolbox which was published by Lee et al. (2012) at PhysioNet in 2016, to obtain results of fixed bining and KDE methods.

2.2.3.1. Fixed Bining (Ranking)

Kaiser, A. and Schreiber, T. (2002) introduced the fixed-bin method, where a specific time series is quantified by splitting the dynamic range into equally sized bins. The ranking is the TE estimation method to get PDFs in (2.9). We compounded the ordinal sample with ranking to improve robustness versus scattered patches and outliers in the underlying distribution. The data set values in X and Y are substituted with their ranks and sorted X and Y in the ordinal sample. The rankings are integers ranging from 1 (lowest value) to N (highest value). Assume $A = \{a_1, a_2, \dots, a_N\}$ and $B = \{b_1, b_2, \dots, b_N\}$ are the transformed series of X and Y respectively.

Thus, concerning A and B, (2.9) may be described by the equation:

$$T_{A\to B} = \sum p(b_{n+1}, b_n, a_n) \log \frac{p(b_{n+1}, b_n, a_n)p(b_n)}{p(b_{n+1}, b_n)p(a_n, b_n)} \quad (2.10)$$

The fixed-bin techniques estimate as follows and in each dimension, R, the same number of bins are used.

$$T_{A\to B} \approx \sum_{u=1, v=1, z=1}^{R} \frac{D_{u,v,z}}{P} \log \frac{D_{u,v,z} D_v}{D_{v,z} D_{u,v}} \quad (2.11)$$

where u, v, z index bins along, b_{n+1}, b_n, and a_n, in order. The number of points in one-dimensional bins' intersection denoted by $D_{u,v,z}$, $D_{u,v}$, and $D_{v,z}$, number of data points in the vth bin of the b_n dimension is D_v. Also, the total number of triplets of b_{n+1}, b_n, and a_n is P.

2.2.3.2. Kernel Density Estimation (KDE)

Rosenblaat (1956) and Parzen (1962) were the first on publishing kernel density estimators. The PDF is calculated in KDE by adding individual distributions which are placed at the center of every data point. The form of individual distributions is determined by a selected kernel and the magnitude of it declines as the range from the distribution's center rises. By normalizing the following, the joint probability at a random point $(\ddot{x}_{i+1}, \ddot{x}_i, \ddot{y}_i)$ in three-dimensional domain x_{i+1}, x_i, y_i may be estimated:

$$p(\ddot{x}_{i+1}, \ddot{x}_i, \ddot{y}_i) \approx \frac{1}{P} \sum_{t=1}^{P} \frac{1}{w_{x_{i+1}} w_{x_i} w_{y_i}} \mathrm{K}\left(\frac{\ddot{x}_{i+1} - x_{i+1,t}}{w_{x_{i+1}}}\right) \mathrm{K}\left(\frac{\ddot{x}_i - x_{i,t}}{w_{x_i}}\right) \mathrm{K}\left(\frac{\ddot{y}_i - y_{i,t}}{w_{y_i}}\right) \quad (2.10)$$

Here, the dimension specified in the subscript bandwidth is w and t indexes the P data points. Then, the formula of the bandwidth:

$$w = 1.06\alpha\hat{\sigma}\, P^{-\frac{1}{5}} \tag{2.11}$$

Here $\hat{\sigma}$ is the sample standard deviation and α is a multiplier for scaling. There are different possible kernels in terms of K but Gaussian kernel was used in this chapter and it is identified as below:

$$K(r) = \frac{1}{\sqrt{2\pi}} e^{-0.5r^2} \tag{2.12}$$

2.3. Data

USD/CHF, USD/GBP, USD/CAD, and USD/EUR, prices obtained from the Investing.com website. The exchange rates were analyzed between 01/01/2010 and 03/12/2020 for WTC and TE methods.

2.4. Results

The aim of this chapter studied the information flows between major exchange rates. The TE results among exchange rates from 01/01/2010 and 03/12/2020 are shown in Figures 12 and 13, and the numerical TE values for 10 year period are submitted in Tables 5 and 6. The TE in coherent zones for every pair is also presented in Table 7.

In all time periods, there is an information flow from USDGBP to other exchange rates in both Ranking and KDE methods (Tables 5 and 6). In Tables 5 and 6, the information flow is measured from row to column. In Table 5, $TE_{EUR\text{->}GBP}$ is 0.9506 and $TE_{GBP\text{->}EUR}$ is 1.0295, which implies that information flow from USDGBP to USDEUR. If we analyze the other TE results with every pair USDGBP have higher TE values in every pair this means USDGBP dominates the others. In Table 6 for the KDE method again $TE_{GBP\text{->}\ldots..}$ showed higher values. On the other hand, if we compare $TE_{CHF\text{->}\ldots..}$ and

$TE_{....->CHF}$ for four pairs USDCHF had smaller values, so we conclude that information flow is from all exchange rates to USDCHF.

For all periods, the daily TE is obtained by Ranking and KDE methods for every exchange rate pair in Figures 12 and 13. The results are present bidirectional information flows between them and shown in blue and red lines. The KDE is a more convenient method since firstly in the Ranking method the TE values and information flows couldn't be obtained clearly because they show exactly the same values for both lines and we couldn't detect very well which line was above or below in each period. Secondly, in the KDE method, the picture is clearer, values are easier to understand and it is easier to interpret which line is above or below and thirdly the KDE methods give us the lower TE values if we compare Table.5 and Table.

Figures 12 and 13, show that the information flow is from USDGBP to other exchange rates as the results in Tables.5 and 6. However, when compared to USDCAD and USDCHF, USDEUR is more influential. According to Figures .13 b,d,f the $TE_{GBP->....}$ line has higher values than the $TE_{....->GBP}$ line over the entire period. This means USDGBP dominates and is effective on others.

Table 5.

Information flow of Exchange Rates by Transfer Entropy Ranking Method

	USDEUR	USDCHF	USDGBP	USDCAD
USDEUR	0.0000	1.1106	0.9560	1.0268
USDCHF	1.0827	0.0000	1.1428	1.0296
USDGBP	1.0295	1.4413	0.0000	1.1180
USDCAD	1.0015	1.3248	1.0167	0.0000

Table 6.

Information flow of Exchange Rates by Transfer Entropy KDE Method

	USDEUR	USDCHF	USDGBP	USDCAD
USDEUR	0.0000	0.0806	0.0791	0.0927
USDCHF	0.0465	0.000	0.0789	0.0834
USDGBP	0.0924	0.0851	0.000	0.0993
USDCAD	0.0870	0.1041	0.0789	0.000

According to the results of Tables 5 and 6 and Figures 12 and 13, USDGBP dominates others. USDGBP is the first one to start trading, followed by USDEUR, USDCAD, and USDCHF is the last of the day. USDGBP was first and USDCHF was always the last one to receive the information under the conditions.

In a financial crisis, the financial time series shows the same characteristics and they co-move in that periods. We studied the co-movement of exchange rates by WTC and according to TE results we aim to show the information flow on the financial crisis period. Because we believe in financial shocks (coherence areas in WTC figures) the information flow is an important indicator for portfolio diversification and investing. From Figure 14 to Figure 19 we analyzed the WTC of exchange rates, TE measurements of them in corresponding coherence periods, and also COVID periods. The COVID period is the last financial crisis, for this reason, we also add this period to our TE measurement because we want to show the relation of exchange rates in special crisis, COVID period, to give ideas for future studies.

Figure 12

Transfer Entropy Analysis by Ranking for USDEUR, USDCHF, USDGBP, USDCAD.

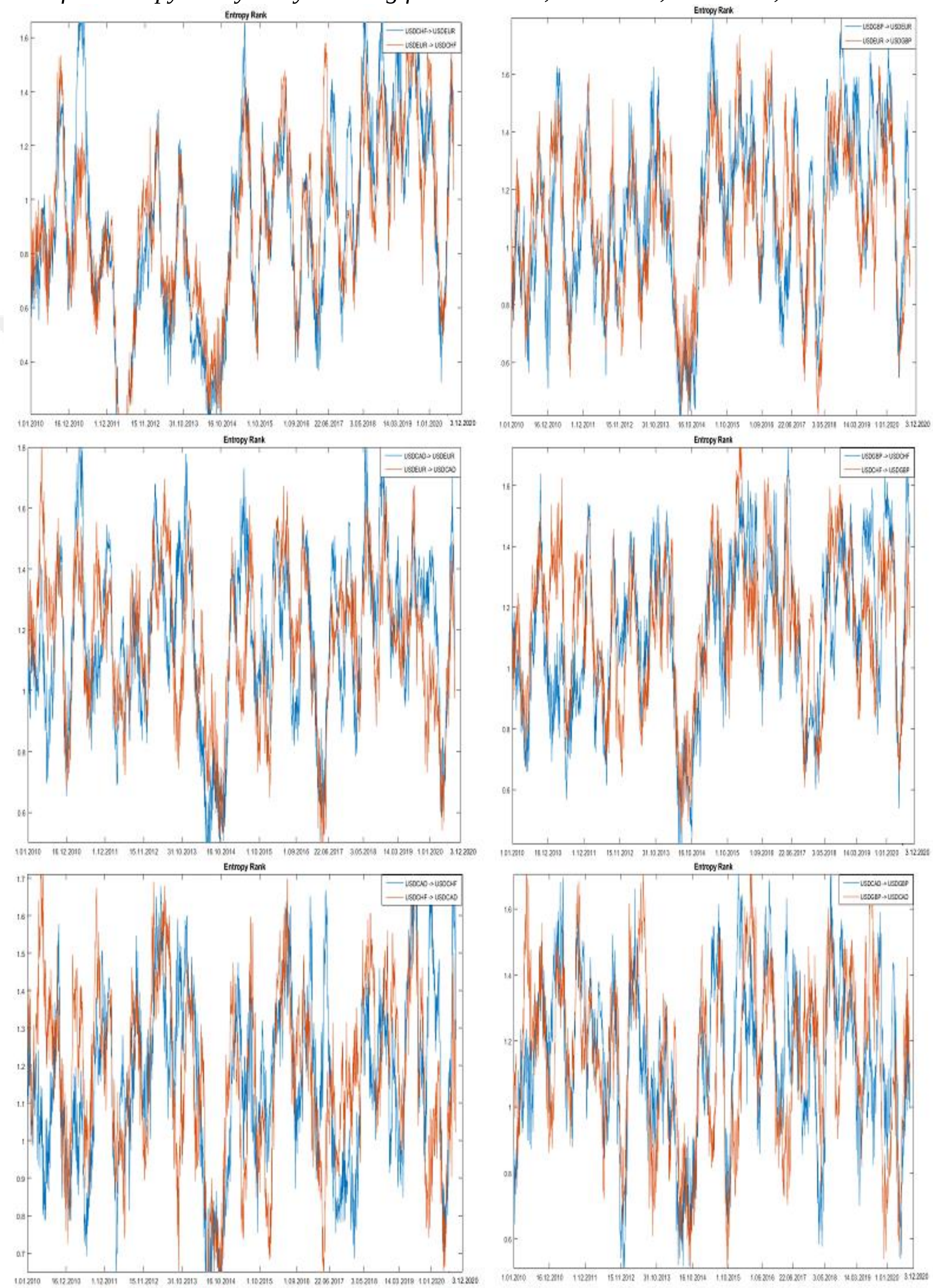

Figure 13

Transfer Entropy Analysis by KDE for USDEUR, USDCHF, USDGBP, USDCAD.

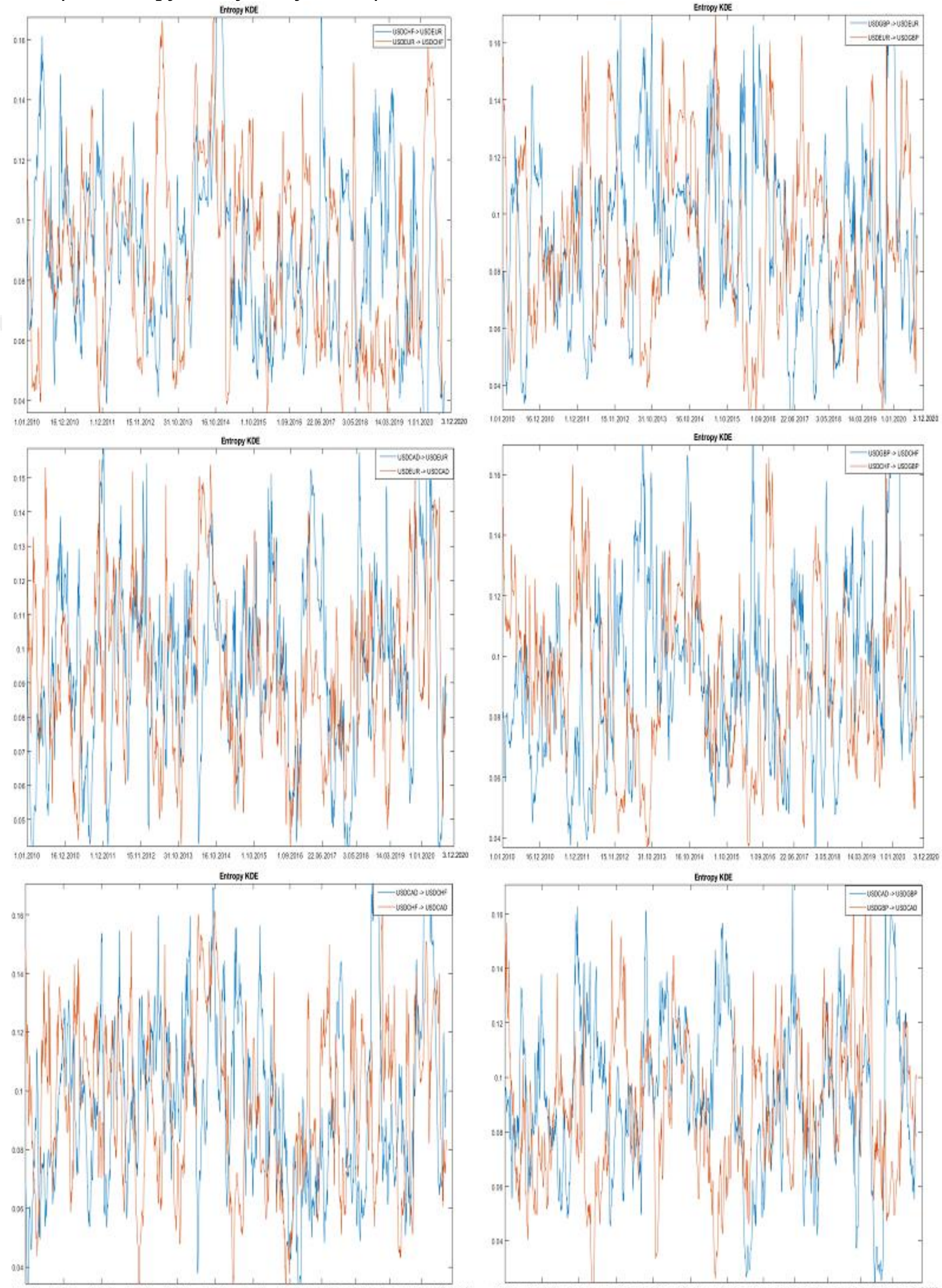

Figure 14

1. WTC USDEUR-USDCHF, 2. TE KDE USDEUR-USDCHF on 1.12.2011- 3.05.2018, 3. TE KDE USDEUR-USDCHF on COVID period

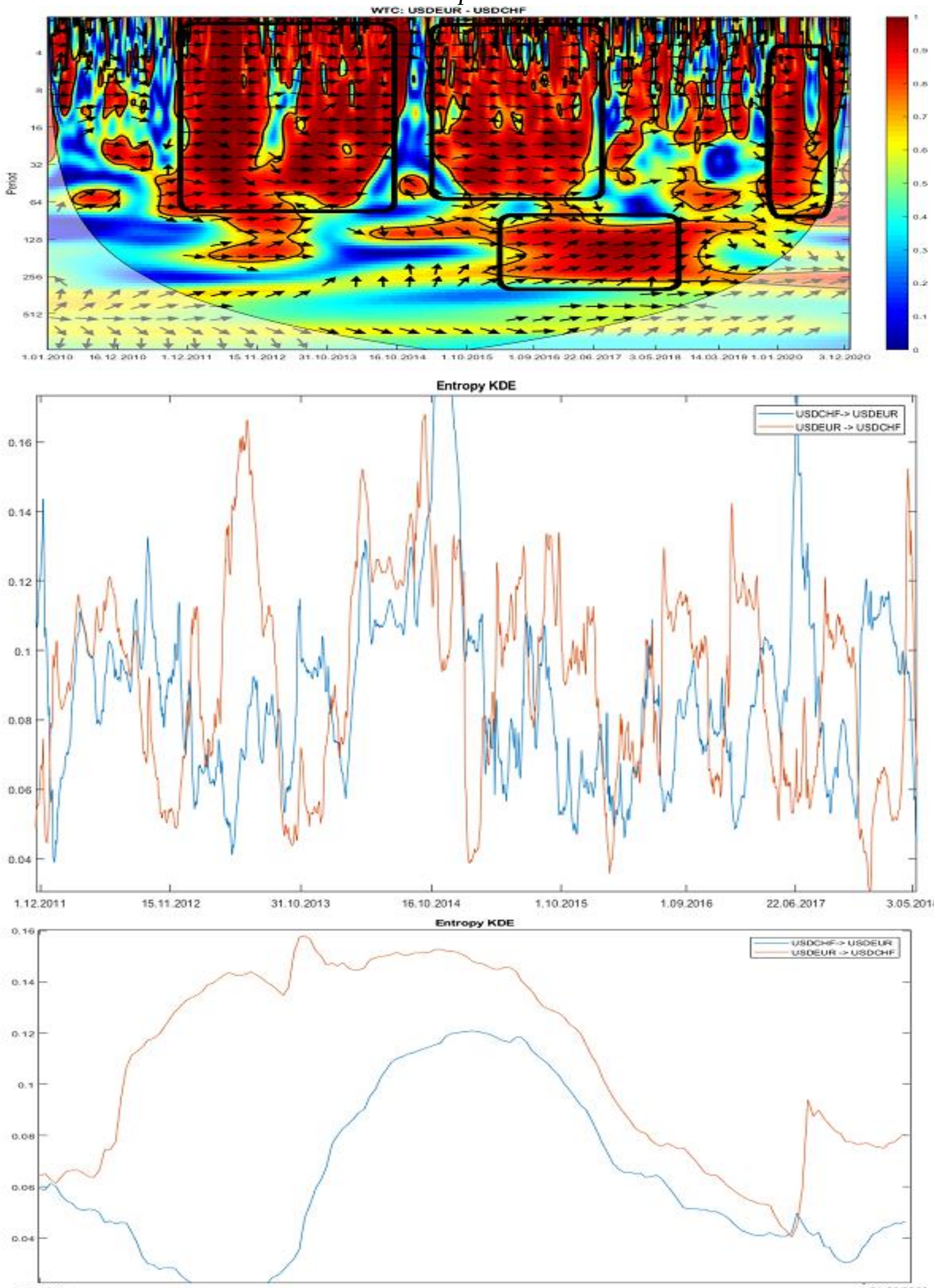

Figure 15

1.WTC USDEUR-USDGBP, 2.TE KDE USDEUR-USDGBP on 16.12.2010 -1.09.2016, 3.TE KDE USDEUR-USDGBP on COVID period

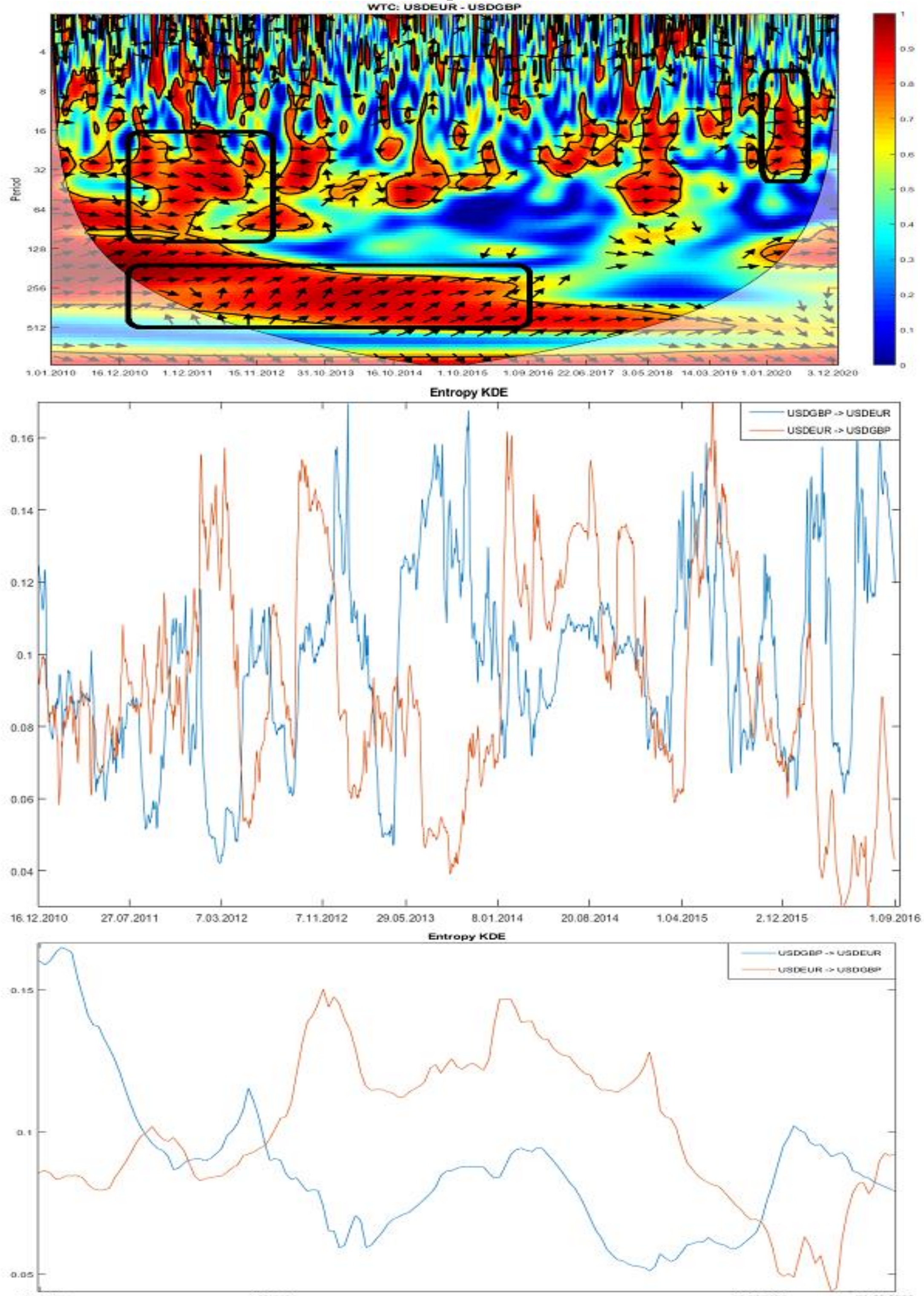

In Figure 14.1 the co-movement areas are represented as black lines. The coherence dates between 1.12.2011-3.05.2018 and on COVID period after 1.1.2020 till 31.08.2020. To understand the information flows we use the TE KDE approach on coherence areas. We can easily see that in Figure 14.2., for all periods $TE_{EUR\text{->}CHF}$(red line) higher(above) than the $TE_{CHF\text{->}EUR}$(blue line) it means information flows is from USDEUR to USDCHF. This result can be supported by the WTC figure since the arrow direction is downwards in all dates except the area between 22.06.2017 and 3.05.2018, which is also seen on the right of the entropy KDE figure as the blue line above the red line. If we analyze the COVID period USDEUR dominates the USDCHF in Figure 14.3. (red line above the blue line) and on WTC the arrows move down for the COVID period.

Figure 15.1, the coherence dates between 16.12.2010 -1.9.2016 and on COVID period after 1.1.2020 - 31.8.2020. From Figure 15.2, after 7.11.2012 (we predict the effect of 6.11.2012 when Obama was elected President of US) usually $TE_{GBP\text{->}EUR}$ (blue line) higher (above) than the $TE_{EUR\text{->}GBP}$ (red line) it means information flows is from USDEUR to USDGBP until 7.11.2012 and then the reverse flow. This result can be supported by the WTC figure, since the arrow directions are downward until 15.11.2012, and then the direction change to upwards. USDEUR dominate the USDGBP on Figure.15.3, between 4.03.2020 (after FED decrease the interest rate 3.03.2020) and 10.07.2020 but on WTC arrows move down and up for COVID period. We could conclude that the information flows change with different dates but generally the flows from USDEUR to USDGBP.

Figure 16

1.WTC USDEUR-USDCAD, 2. TE KDE USDEUR-USDCAD on 1.12.2011-3.10.2013 3.TE KDE USDEUR-USDCAD on COVID period.

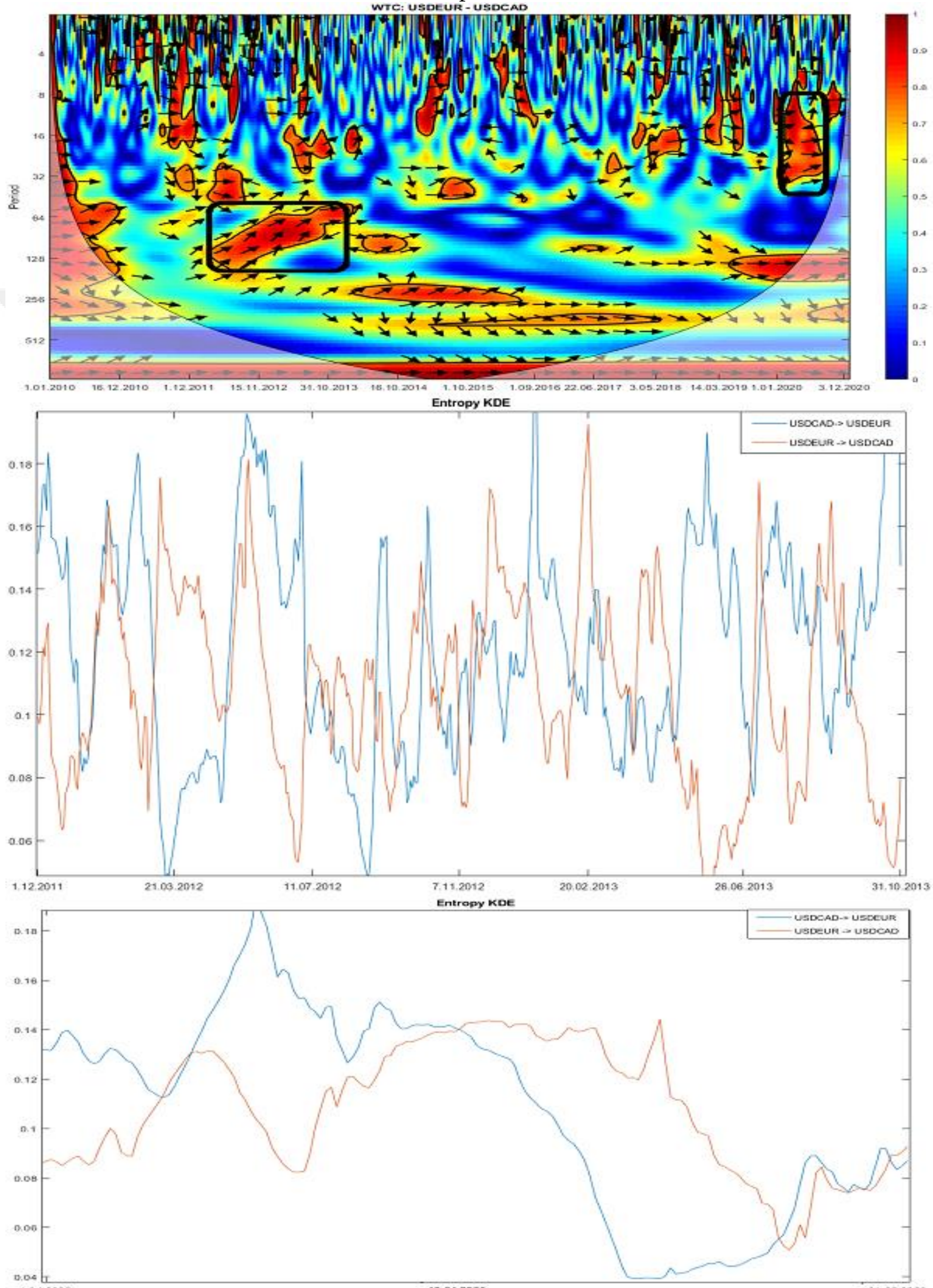

Figure 17

1.WTC USDCHF-USDGBP, 2. TE KDE USDCHF-USDGBP on 1.12.2011-31.10.2013, 3.TE KDE USDCHF-USDGBP on COVID period

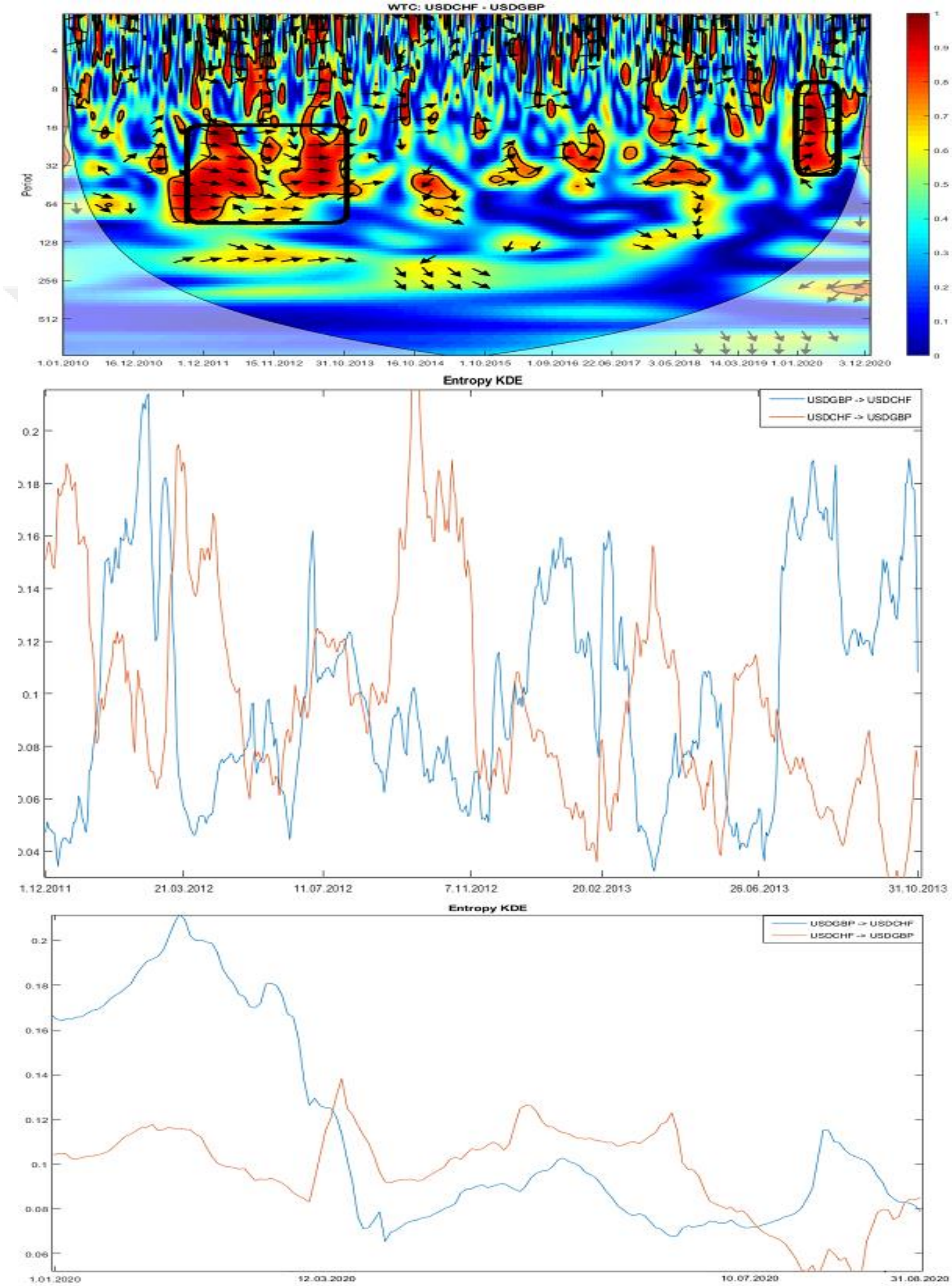

Figure 16.1 the co-movement areas are represented as black lines. The coherence dates between 1.12.2011-3.10.2013 and on COVID period after 1.1.2020 till 31.08.2020. We obtain on Figure 16.2, $TE_{EUR\text{->}CAD}$ (red line) usually shows us lower values than $TE_{CAD\text{->}EUR}$ (blue line), namely, information flows is from USDCAD to USDEUR as can be seen in Table 7, since $TE_{CAD\text{->}EUR}$ > $TE_{EUR\text{->}CAD}$. On the WTC figure, the arrow direction upwards in brief USDCAD dominates the USDEUR. This shows that we reach the same result with the two methods. If we analyze the COVID period USDEUR dominates the USDCAD after 16.04.2020 on Figure 16.3. and on WTC the arrows move down and up for the COVID period. We couldn’t conclude the clear information flows because it doesn’t represent a fixed direction for the whole period but at a specific time, we could.

The co-movement areas between 1.12.2011-31.10.2013 and on COVID period after 1.1.2020 till 31.08.2020 in Figure 17.1. In Figure 17.2., Although it has a high value in certain periods before 7.11.2012, especially after this date, $TE_{GBP\text{->}CHF}$ is higher than $TE_{CHF\text{->}GBP}$, so information flows is from USDGBP to USDCHF after 7.11.2012. This is also consistent with the result $TE_{GBP\text{->}CHF}$ =0.1081 > $TE_{CHF\text{->}GBP}$ =0.0721 in Table 3 and also by WTC it can also be seen, arrow directions changed after 15.11.2012 downwards to upwards. If we interpret Figure 17.3. USDGBP dominates the USDCHF except period 12.03.2020 (we predict the effect of COVID was announced pandemic: 11.3.2020) – 10.07.2020 and on WTC the arrows look like they were pointing up for COVID period in other words USDGBP is on the leading side except for four months which are shown in Figure 17.3.

Figure 18

1.WTC USDCHF-USDCAD, 2. TE KDE USDCHF-USDCAD on 16.12.2010-15.11.2012, 3.TE KDE USDCHF-USDCAD on COVID period

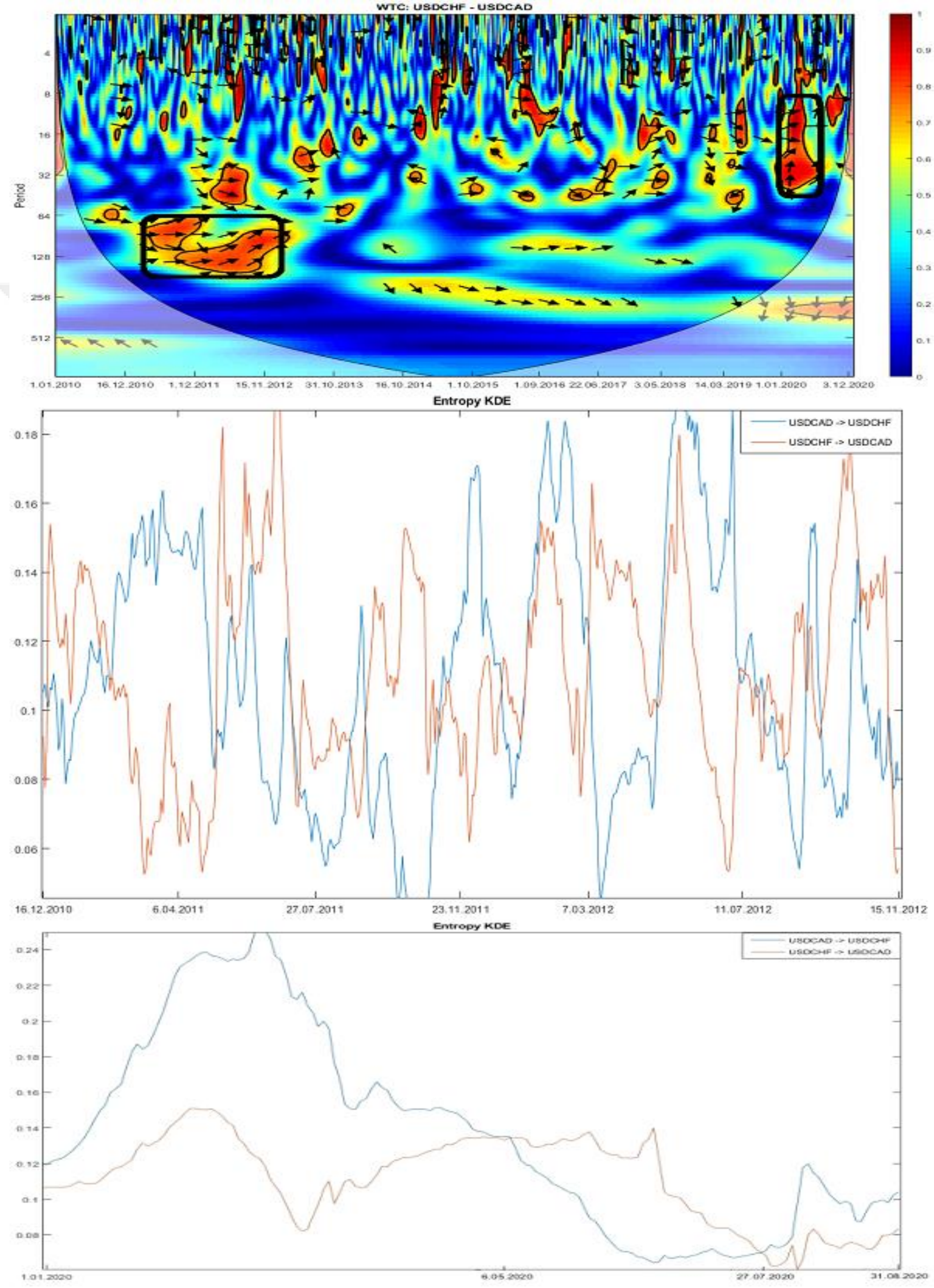

Figure 19

1.WTC USDGBP-USDCAD, 2. TE KDE USDGBP-USDCAD on 1.12.2011-1.10.2015, 3.TE KDE USDGBP - USDCAD on COVID period

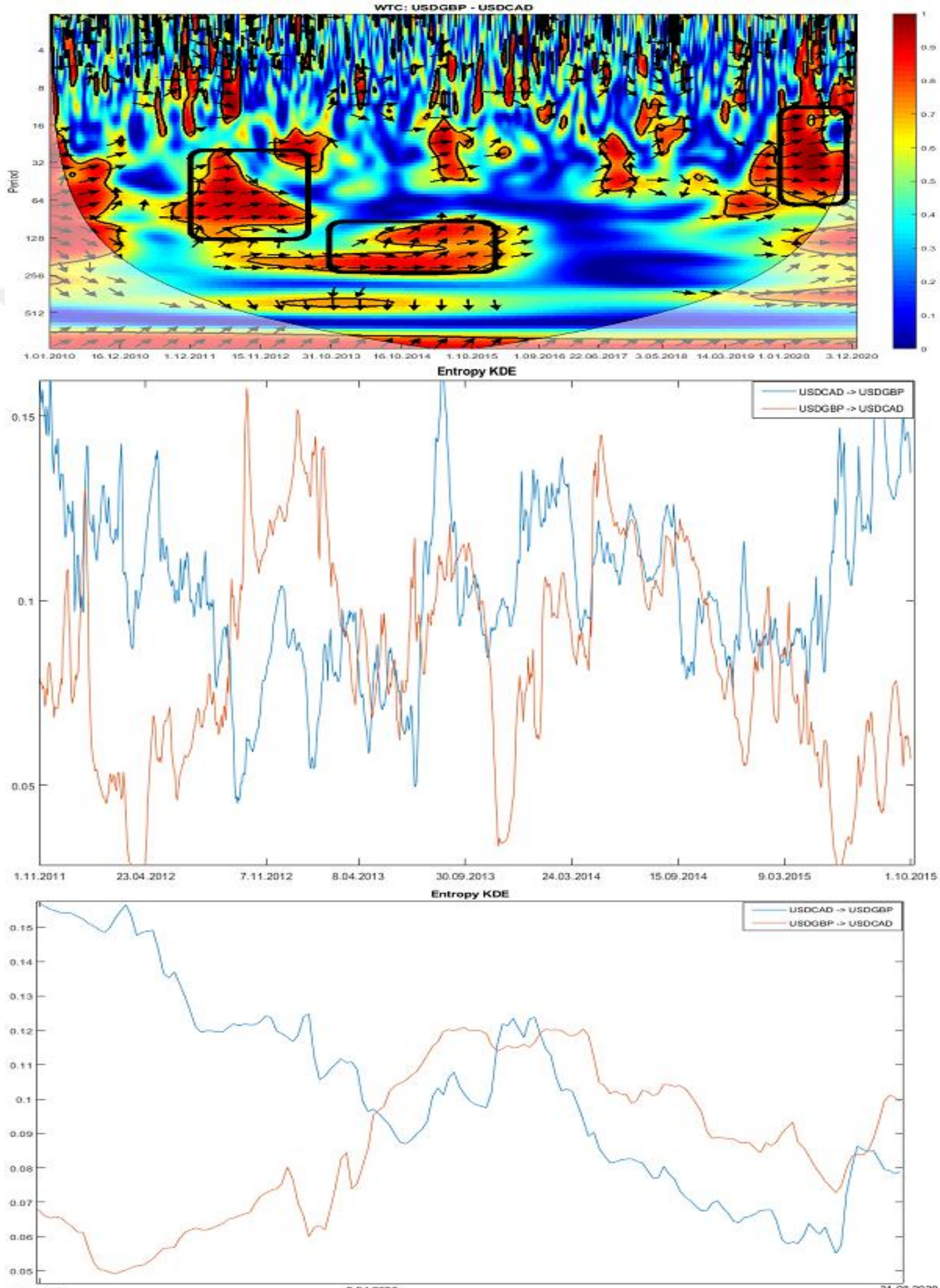

In Figure 18.1, the coherence dates between 16.12.2010-15.11.2012 and on COVID period after 1.1.2020 till 31.08.2020 for USDCHF-USDCAD. We see that in Figure 18.2, it is an information flow from $TE_{CAD->CHF}$ to $TE_{CHF->CAD}$ (blue line above the red line) for some time intervals. In Figure 18.1, since arrow direction upwards, USDCAD leading the USDCHF and $TE_{CAD->CHF}$: 0.0794 higher than $TE_{CHF->CAD}$ value on Table 7. In the light of these findings, USDCAD affects USDCHF on coherence periods. On COVID period $TE_{CAD->CHF}$ bigger than $TE_{CHF->CAD}$ except 6.5.2020-27.7.2020 and also in Figure 18.1., the arrows point up after 1.1.2020 so, USDCAD dominates the USDCHF on the COVID period.

If we interpret Figure 19.1, the coherence dates between 1.12.2011-1.10.2015 and on COVID period after 1.1.2020 till 31.08.2020. If we look at Figure 19.2, most of the entire coherence period $TE_{CAD->GBP}$ higher than the $TE_{GBP->CAD}$ it means information flows is from USDCAD to USDGBP in this period. This result can be supported by WTC figure and Table 7, since in general arrow direction upwards Figure 19.1 and Table 7, $TE_{USDGBP>USDCAD}$:0.0571 and $TE_{USDCAD>USDGBP}$:0.1145 which states that USDCAD dominates the USDGBP for coherence times. In the COVID period, USDGBP dominates the USDCAD in Figure 19.3 (red line above the blue line) after 2.04.2020 and on WTC the arrows move up and down for the COVID period, so until 2.04.2020 USDCAD was on the leading side but after this day the position was changed.

In Table 7, we interpreted TE values for every bidirectional pair in correspondence coherent times and bold text represents the higher TE values of one than the other. According to this, It is seen that USDCAD dominates other exchange rates in the coherence periods obtained by WTC analysis. Also, there is more information flow to USDCHF from other exchange rates.

2.5. Conculusion

In this chapter, we examine the co-movement of exchange rates which are USDEUR, USDCHF, USDGBP, and USDCAD through WTC, and information flow between them by TE measure. Here, we have stated that TE can detect the information flow in directional coupling between two exchange rates. It can help us to see the direction of the net flow.

Table 7

Information flow of Exchange Rates by Transfer Entropy on Coherent Dates

Coherent Dates	TE values for Every Bidirectional Pair	
01.12.2011 - 03.05.2018	$\mathbf{TE_{USDEUR->USDCHF} : 0.1136}$	$TE_{USDCHF->USDEUR}$: 0.0691
16.12.2010 - 01.09.2016	$TE_{USDEUR->USDGBP}$: 0.0431	$\mathbf{TE_{USDGBP->USDEUR} : 0.1196}$
01.12.2011 - 31.10.2013	$TE_{USDEUR->USDCA}D$: 0.0799	$\mathbf{TE_{USDCAD->USDEUR} : 0.1474}$
01.12.2011 - 31.10.2013	$TE_{USDCHF->USDGBP}$: 0.0721	$\mathbf{TE_{USDGBP->USDCHF} : 0.1081}$
16.12.2010 - 11.11.2012	$TE_{USDCHF->USDCAD}$: 0.0542	$\mathbf{TE_{USDCAD->USDCHF} : 0.0794}$
01.11.2011 - 01.10.2015	$TE_{USDGBP->USDCAD}$: 0.0571	$\mathbf{TE_{USDCAD->USDGBP} : 0.1145}$

WTC detected the financial crisis or coherence periods in the time-frequency domain and we interpreted rise and fall in the information transfer and direction of it during these periods by TE. After WTC analysis, coherence areas are used for TE measure. When we compare the WTC and TE figures we face congruence results. WTC and TE outcomes support each other. When the arrow directions change in WTC figures, at the same time we see a change of direction in the lines on the TE graphs.

We used Fixed Bins (Ranking) and KDE methods for TE measure and compared their performance. When we compared KDE gives more interpretable results. We conclude that USDGBP was the most influential exchange rate and USDCHF is the most dominated for 10 year period. During the coherence periods, USDCAD took the information in firstly and dominated the others.

Last year, we faced the worst crisis ever which was COVID. In WTC figures we can easily see that all exchange rates showed high co-movements in this period and we also analyse the information transfer ın that time. According to the results, USDEUR was in the leading position and the information flow was in a bidirectional way in other pairs for the COVID period.

In this chapter three different results are obtained: 1) USDGBP is on the leading side, 2) USDCAD dominates other exchange rates on coherent periods and, 3) Kernel Density Estimation (KDE) method could lead to better results. Furthermore, we have improved the TE methods by considering the co-movement of time series and we showed TE with WTC analysis indicate, phase angle direction change in WTC describe TE flow change. WTEGTM allows us to capture the change in the causality and direction of net information flow between nonlinear and nonstationary time series simultaneously, especially in times of financial crisis like in the COVID period. These two methods give equivalent and correct outputs in coherence times. In the future, this method can be used to anticipate risk in times of crisis like COVID. Therefore, we interpret these results as the investors adjust their portfolio positions for exchange rates in financial crisis periods.

CHAPTER 3 CAUSALITY, INFORMATION FLOW, AND CO-MOVEMENT ANALYSIS OF MAJOR STOCK INDICES

Summary

Stock indices are key indicators of the economy since they indicate the strength of a country's stock market. For this reason, causality, information flow, and co-movement analysis of stock indices gain importance to compare the economies of countries. Here, in wavelet coherence (WTC) analysis, the co-movement between stock indices provided and coherent areas can be shown and information flow is indicated for five years periods and especially on coherent zones by Transfer Entropy(TE), which detects cause and effect relations. In this chapter, we analyzed the information flow and co-movement among FTSE100 in the United Kingdom, the DAX in Germany, and S&P500 Index in the United States stock indices. Three different results are obtained: 1) DAX is on the leading side in general for 5 year periods, 2) Bidirectional information flows arise for every pair in the coherent periods, and 3) TE guided WTC analysis shows, TE sign change can be explained by phase angle direction got with WTC. These results indicate both methods yield proper outcomes in coherent time zones and financial crisis times like the COVID period which we have faced for two years, for this reason, the results were also obtained for the COVID period and in general, that shows DAX dominated other indices. We published this thesis to help investors avoid risk in their stock portfolios, especially during financial crisis periods

3.1. Introduction and Literature Review

In finance, a stock index represents the stock market, which allows investors to compare existing prices with historical prices to determine market performance. The value of the stock index is measured by the prices of stocks in it. The value of an index in a country could be an important indicator of the economic situation, shows the strength of a country's stock market in a given nation, indicates investor perception about the country's economy, and helps to predict future situations. Therefore, the relationship between stock indices is very important. We considered daily values of stock indices for information flow and co-movements between them. The interaction between stock indices will be higher in or after the financial crisis (Jiang et al., 2017). For this reason, We aim to demonstrate the quantitative methods for connection and innovation of stock indexes and show co-movement among them by WTC and information flows with TE in crisis periods.

There are several methods for measuring the information flows between time series. The most popular technique is Granger causality (Granger, 1969) used to explain causal relations between time series. Granger causality is extended in a non-linear way by Transfer Entropy (Barnett et al. 2009). Transfer entropy proposed by Schreiber (2000), detects the bidirectional information flow among two-time series and information quantity. It is derived from Shannon entropy (Shannon, 1948). If we compared with the mutual information, TE takes the dynamics of information transfer into account and the direction of flow more explicitly. TE has been applied in a lot of areas. Ver Steeg (2012) used this method for social media. Lee et al. (2012) detect the direction coupling change in biomedical time series. Sumioka et al. (2007) used TE on physiological time series. In the area of finance, Yao and Li (2020) investigated information flow between EPU (Economic Policy Uncertainty), stock market, and investor sentiment by Effective Transfer Entropy which was proposed by Sensoy et al. (2014), they explored the information flow among stock markets and exchange rate. Teng and Shang (2017) extended the TE coefficient for quantifying the level of information flow between financial time series. He and Shang (2017) compared the TE methods for financial time series. Mohaghegh et al. (2021) used the TE approach to analyze the Iranian stock exchange's financial crisis and compared it to the Dow Jones financial market and Park et al. (2021) studied information flows among financial assets and bitcoin prices. Mendoza Urdiales RA et al (2021) measured the information flow among stock prices and social media with TE.

Wavelet coherence is a method to detect co-movement among time series. Torrence and Compo (1998) defined coherence and cross-wavelet spectra concentrated on atmospheric time series. WTC and cross wavelet transformation methods for two-time series, concentrating on wavelet analysis presented by Grinsted et al. (2004). The use of phase angle statistics was demonstrated in their research to analyze reliance on causal relationships. Tiwari (2012) investigated the connections between interest rates and prices of shares in the Indian economy and inflation, industrial production, and price of oil in the German economy using a cross-wavelet approach. Goodell and Goutte (2021) analyzed the co-movement between COVID-19 deaths and Bitcoin via WTC analysis. Özdurak, C. and Karataş, C. (2021) analyzed the co-movements of the biggest technological stocks, FAANG and Microsoft, to see if there was a new technological bubble in the market. Karatas, C. and Unal, G. (2021) examined exchange rate co-movements through WTC and their fractal behavior. Gherghina, Ş. C., and L. N. Simionescu., (2021) studied the stock market returns-COVID-19 interdependence with WTC analysis.

In recent years, a lot of studies examining the relationship of time series with each other have been applied in the academic literature. Most of the research was focused on understanding the cause-and-effect relationship between the series. For example, Ongan and Gocer (2017) examined the causal relationships among the US stock indices and EPU index. Especially in periods of the financial crisis, besides this cause-effect relationship, the information flow and direction between the stock prices gain importance. As a result of this necessity, in this chapter, we determined the coherence times when the stock indices moved together by using WTC, and then we investigated the net information flow direction in this period by using the TE method and made nonlinear and nonstationary experiments of stock index and we named this analysis as Wavelet Transform Guided Transfer Entropy Method (WTGTEM).

WTGTEM is a nonlinear generalization of the continuous wavelet transform causality method which was proposed by Olayeni (2016) and as distinct from this method, TE through WTC method shows, phase angle leading direction change obtained with WTC explain TE sign change. In this methodology, the bidirectional causality and coherence zones between time series in the time-frequency domain are detected by wavelet coherence and guided by this analysis the information quantity transferred and the bidirectional information flow between time series measured by TE. Unlike Granger Causality, TE detects the quantitative direction of information flow and asymmetric qualitative information transfer. WTEGTM allows us to capture the change in the causality and direction of net information flow between the two non-linear and non-stationary time series simultaneously, especially in financial distress periods.

Section 2 starts with Wavelet Transform Guided Transfer Entropy Method (WTGTEM). Section 3 discusses the outputs of WTC and TE and in conclusion, we interpret the results and gains of this chapter.

3.2. Methodology

3.2.1. Wavelet Transform Guided Transfer Entropy Method (WTGTEM)

In this chapter again we proposed Wavelet Transform Guided Transfer Entropy Method (WTGTEM). Firstly, we determined the coherence zones when the stock indexes moved together and their cause and effect relation through WTC, and then we investigated the direction of the net information flow in this period by using the TE method.

3.2.2. A Summary of Wavelet Coherence (WTC)

In this thesis, the co-movement of stock indices is investigated. If they co-move, there are coherent areas in WTC plots that are shown as red to blue colors, representing high to low degree coherence at a private timeframe.

The Cross Wavelet Transform (XWT) is created by combining two CWTs (Continuous Wavelet Transforms). XWT displays the mutual strength and relative phase of time series in frequency-time space. The phase difference between stock indices explains the causal relations.

CWT defined as;

$$W_x(\tau, s) = \frac{1}{\sqrt{s}} \sum_{t=1}^{N} x(t) \varphi^* \left(\frac{t-\tau}{s} \right) \tag{3.1}$$

Here * is a complex conjugate.

Morlet Wavelets;

$$\varphi(\eta) = \pi^{-1/4} e^{i\omega_0 \eta} e^{-1/2\eta^2} \tag{3.2}$$

here η is time, and ω_0 is frequency chosen 6 because it offers a strong match among frequency and time domain [Grinsted et al., 2004].

$W_n^X(s)$, W_n^Y(s); wavelet transforms of X, Y, and their XWT is;

$$\Psi_n^{XY}(s) = W_n^X(s).W_n^{Y*}(s) \tag{3.3}$$

Here, $W_n^{Y*}(s)$ is complex conjugate of $W_n^Y(s)$.

So one can define the wavelet coherence (WTC) as;

$$R_n^2(s) = \frac{|S(\ s^{-1}\Psi_n^{XY}(s)\ )|^2}{S(\ s^{-1}|W_n^X(s)\ |^2).S(\ s^{-1}|(W_n^Y(s)\ |^2)} \tag{3.4}$$

Here S is smoothing operator, s is a wavelet scale.

3.2.2.1. Phase

WTC' phase difference is;

$$\varphi_{xy}(u,s) = tan^{-1}\left(\frac{I\{S((s^{-1}\Psi_n^{XY}(u,s)))\}}{R\{S((s^{-1}\Psi_n^{XY}(u,s)))\}}\right) \quad ,\varphi_{xy} \in [-\pi,\pi] \tag{3.5}$$

Here: R and I; real and imaginary pieces of power spectrum. Phase differences among stock indices tells how they co-move at distinct scales. If the arrows move right, the indices co-moved, so in phase. If arrows move up (phase difference on [0,$\pi/2$]), second lead first. If arrows move down (phase difference on [0,$-\pi/2$]), then the first leading.

3.2.3. A Summary of Transfer Entropy

Shannon published ‘‘Mathematical theory of communication’’ in 1948, it was the first to study Information theory. Probability theory is used for the analysis of information transfer in information theory. It has been utilized in the disciplines of economics, sociology, statistics, biology, etc. after decades of development. The classical information theory is Shannon’s information theory. Shannon’s information theory defines information as the reduction of uncertainty. As a result, we may evaluate information via measuring the decrease in uncertainty.

Shannon entropy is defined as follows:

$$H(X) = H(p_1, p_2, \dots, p_k) = \sum_{k=1}^{K} p_k l(x_k) = \sum_{k} p_k log \frac{1}{P(x_k)} = -\sum_{k} p_k log P(x_k) \quad (3.6)$$

$P(x_k)$ denote the probability of x_k.

Mutual information describes the relation between two data sets, it is information of one variable that has information about the other. Consider $p(x, y)$ is the joint distribution of (X, Y), $p(x), p(y)$ are marginal distributions, so, the relative entropy of product distribution $p(x)p(y)$ and mutual information is $MI(X; Y)$.

$$H(X, Y) = H(X) + H(Y|X) = H(Y) + H(X|Y)$$

$$MI(X; Y) = H(X) - H(X|Y) = H(X) + H(Y) - H(X, Y)$$

$$= \sum_{x} p(x) log \frac{1}{p(x)} + \sum_{y} p(y) log \frac{1}{p(y)} - \sum_{x,y} p(x, y) log \frac{1}{p(x, y)} \quad (3.7)$$

$$= \sum_{x} \sum_{y} p(x, y) log \frac{p(x, y)}{p(x)p(y)}$$

Because of the symmetry of the outcomes, with mutual information, information exchange dynamics is not available and we cannot identify relation among causative and passive ones. TE solved this problem. Transfer entropy (TE) can efficiently separate repulsive elements from responsive elements and discover asymmetry in subsystem interactions. The TE describes the amount of information flow from one variable to another.

The definition of TE is;

$$T_{Y\to X} = H(X_{n+1}|X_n) - H(X_{n+1}|X_n\ ,\ \ Y_n)$$

$$\begin{aligned} T_{Y\to X} &= \left[-\sum p(x_{n+1}, x_n, y_n)\log(p(x_{n+1}|x_n))\right] - \left[-\sum p(x_{n+1}, x_n, y_n)\log\big(p(x_{n+1}|x_n, y_n)\big)\right] \\ &= \sum p(x_{n+1}, x_n, y_n)\log\frac{p(x_{n+1}|x_n, y_n)}{p(x_{n+1}|x_n)} \\ &= \sum p(x_{n+1}, x_n, y_n)\log\frac{p(x_{n+1}, x_n, y_n)p(x_n)}{p(x_{n+1}, x_n)p(x_n, y_n)} \end{aligned} \tag{3.8}$$

and the opposite direction of TE is

$$T_{X\to Y} = \sum p(y_{n+1}, x_n, y_n)\log\frac{p(y_{n+1}, x_n, y_n)p(y_n)}{p(y_{n+1}, y_n)p(x_n, y_n)} \tag{3.9}$$

If the net information flow $T_{X\to Y} - T_{Y\to X} > 0$, it means the information flow from X to Y.

Direction is the advantage of TE. We can deduce that bidirectional information flow is asymmetric according to the TE formula. We could separate the active and passive factors because of asymmetry.

We used Kernel Density Estimation (KDE) method to indicate TE and Matlab toolbox which was published by Lee et al. (2012) at PhysioNet in 2016, to obtain results of KDE method.

3.2.3.1. Kernel Density Estimation (KDE)

Rosenblatt (1956) and Parzen (1962) were the first on publishing kernel density estimators. The PDF is calculated in KDE by adding individual distributions which are placed at the center of every data point. The form of individual distributions is determined by a selected kernel and the magnitude of it declines as the range from the distribution's center rises. By normalizing the following, the joint probability at a random point $(\ddot{x}_{i+1}, \ddot{x}_i, \ddot{y}_i)$ in three-dimensional domain x_{i+1}, x_i, y_i may be estimated:

$$p(\ddot{x}_{i+1}, \ddot{x}_i, \ddot{y}_i) \approx \frac{1}{P}\sum_{t=1}^{P} \frac{1}{w_{x_{i+1}} w_{x_i} w_{y_i}} \mathrm{K}\left(\frac{\ddot{x}_{i+1} - x_{i+1,t}}{w_{x_{i+1}}}\right) \mathrm{K}\left(\frac{\ddot{x}_i - x_{i,t}}{w_{x_i}}\right) \mathrm{K}\left(\frac{\ddot{y}_i - y_{i,t}}{w_{y_i}}\right) \quad (3.10)$$

Here, the dimension specified in the subscript bandwidth is w and t indexes the P data points. Then, the formula of the bandwidth:

$$w = 1.06\alpha\hat{\sigma}\, P^{-\frac{1}{5}} \quad (3.11)$$

Here $\hat{\sigma}$ is the sample standard deviation and α is a multiplier for scaling. There are different possible kernels in terms of K but Gaussian kernel was used in this thesis and it is identified as below:

$$K(r) = \frac{1}{\sqrt{2\pi}} e^{-0.5r^2} \quad (3.12)$$

3.3. Data

In this chapter, we use the major stock indices' daily values, which are the FTSE100 in the United Kingdom, the DAX in Germany, and S&P500 Index in the United States, from the Investing.com website from 4/01/2016 to 5/02/2021 and for COVID period from 02/01/2020 to 30/06/2021 because one of the aims of this thesis show readers the results of WTC and TE on financial crisis periods. We look at the days when the three stock indices run the same time for the compatibility of the data. The daily prices of stock indices are shown in Figure 20 for the analyzed periods.

Figure 20

Daily Prices of S&P500, DAX, and FTSE100 from 4.01.2016 to 5.02.2021

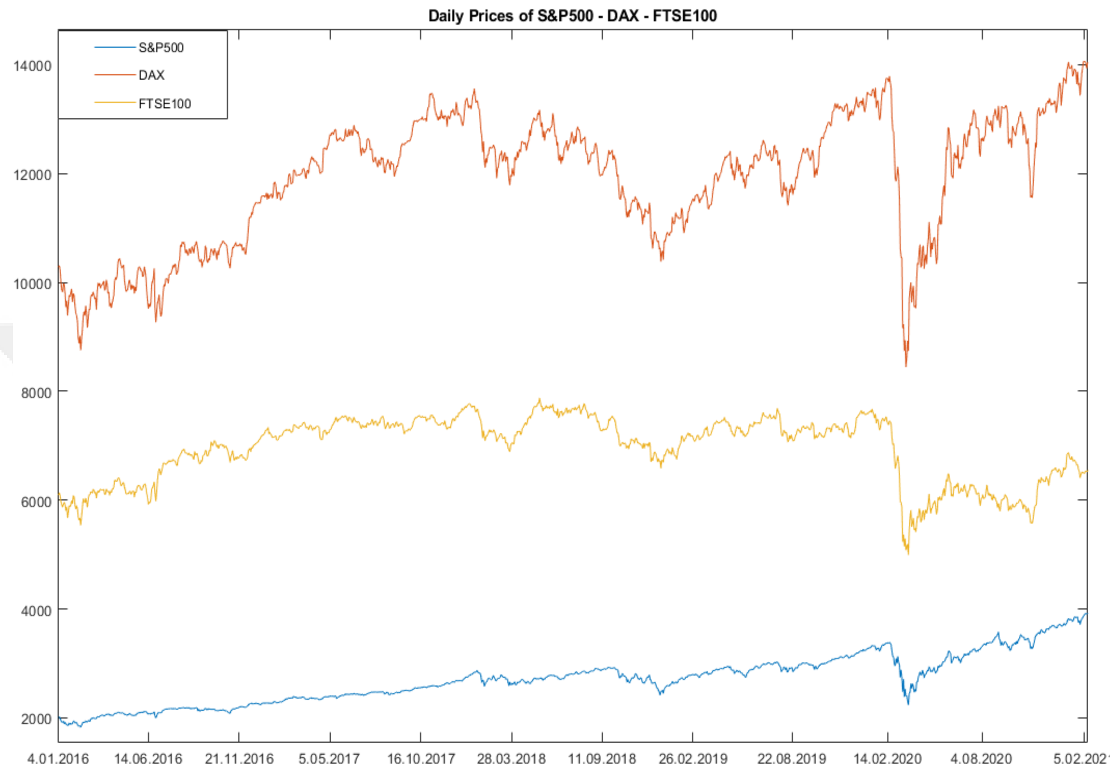

3.4. Results

Table 8

Transfer Entropy Between Stock Indexes

	S&P500	DAX	FTSE100
S&P500	0	0.0831	0.1184
DAX	0.1083	0	0.1214
FTSE100	0.0761	0.0868	0

The aim of this chapter studied the information flows between major stock indices. The TE results among stock indices from 4/01/2016 to 5/02/2021 are shown in

Figures 2, 3, 4, and the numerical TE values for 5 year period are submitted in Table 1. The TE for every pair is presented in Table 2 for coherent zones and in Table 3 for the COVID period.

In all time period there is an information flow from DAX to other stock indices because in Table 8, $TE_{S\&P500\text{->}DAX}$ is 0.0831 and $TE_{DAX\text{->}SP500}$ is 0.1083, which implies that information flow from DAX to S&P500. In Table 8 again $TE_{DAX\text{->}FTSE100}$: 0.1214 showed a higher value this means DAX dominates the others. On the other hand, if we compare $TE_{FTSE100\text{->}SP500}$ and $TE_{SP500.\text{->}FTSE100}$, $TE_{FTSE100\text{->}}$ had smaller values, so we conclude that information flow is from all indices to FTSE100.

Figure 21

Transfer Entropy by KDE for S&P500 and DAX from 4.01.2016 to 5.02.2021.

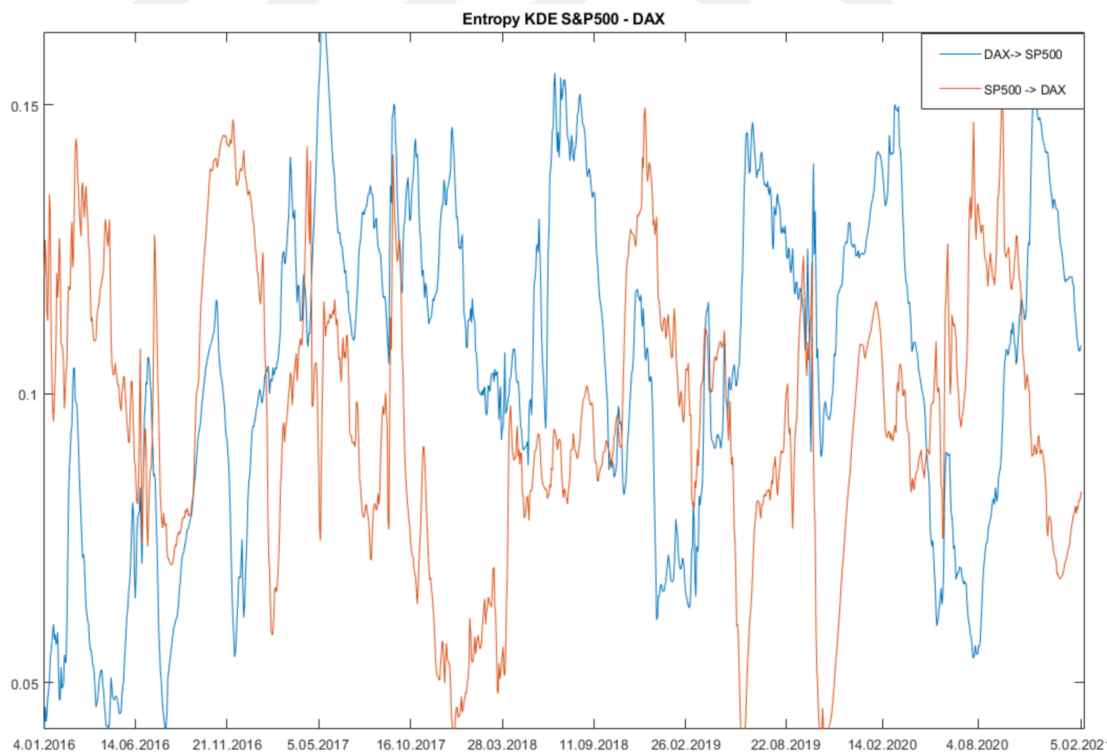

In Figure 21, $TE_{\mathbf{SP500\text{->}DAX}}$ (red line) shows higher values, from 4.01.2016 to 5.05.2017, so SP500 dominates DAX, which claims the same result in the WTC plot of

Figure 24 (The arrows move down means SP500 leads DAX), and after 5.05.2017 $TE_{\mathbf{DAX->SP500}}$ has higher values, and in WTC plot the arrows move up (DAX is on the leading side) for the same time interval, this show that for 4 years period the information flows from DAX to SP500 after 5.05.2017. If we analyze the Table 8 $TE_{\mathbf{DAX->SP500}}$: 0.1083 > $TE_{\mathbf{SP500->DAX}}$: 0.0831, and thus represent the same conclusion SP500 is affected by DAX.

Figure 22

Transfer Entropy by KDE for S&P500 and FTSE100 from 4.01.2016 to 5.02.2021.

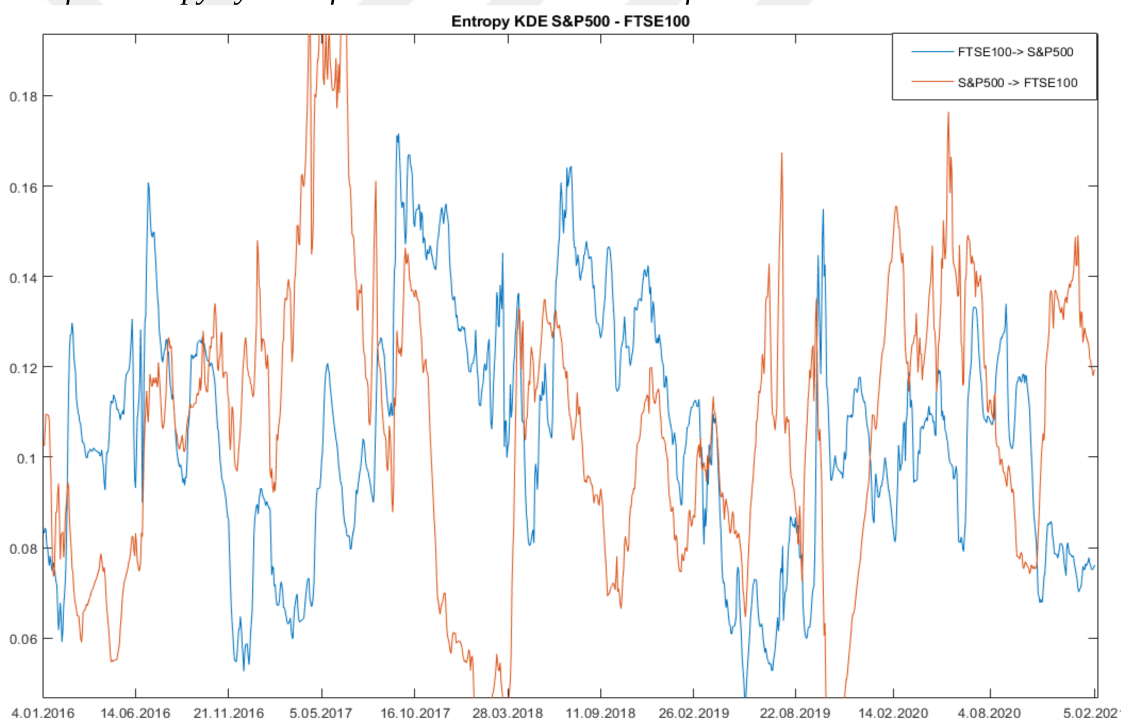

Except for the middle part in Figure 22, the red line is above the blue line, and in Table8, we obtained $TE_{SP500->FTSE100}$: 0.1184 > $TE_{FTSE100->SP500}$: 0.0761, which implies that SP500 dominates FTSE100 except from 16.10.2017 to 26.02.2019. This result was also supported by the WTC plot of Figure 25 (The arrows move up means FTSE100 leads S&P500 from 16.10.2017 to 26.02.2019)

In Figure 23, the blue line is below the red line for almost the entire time range, and in Table8, we showed $TE_{DAX\text{->}FTSE100}$: 0.1214 > $TE_{FTSE100\text{->}DAX}$: 0.0868, so the information flow from DAX to FTSE100. If we analyzed the WTC (DAX-FTSE100) of Figure 26, the direction of the arrows varies on various dates. Therefore, instead of deciding on 5 years, we can decide which stock index is more dominant in certain date intervals.

According to the results of Table 8 and Figures 21, 22 and 23, DAX dominates S&P500 and FTSE100, in other words, DAX is the first one to start trading, followed by S&P500 and FTSE100 for analyzed five-year time interval.

Figure 23

Transfer Entropy by KDE for DAX and FTSE100 from 4.01.2016 to 5.02.2021.

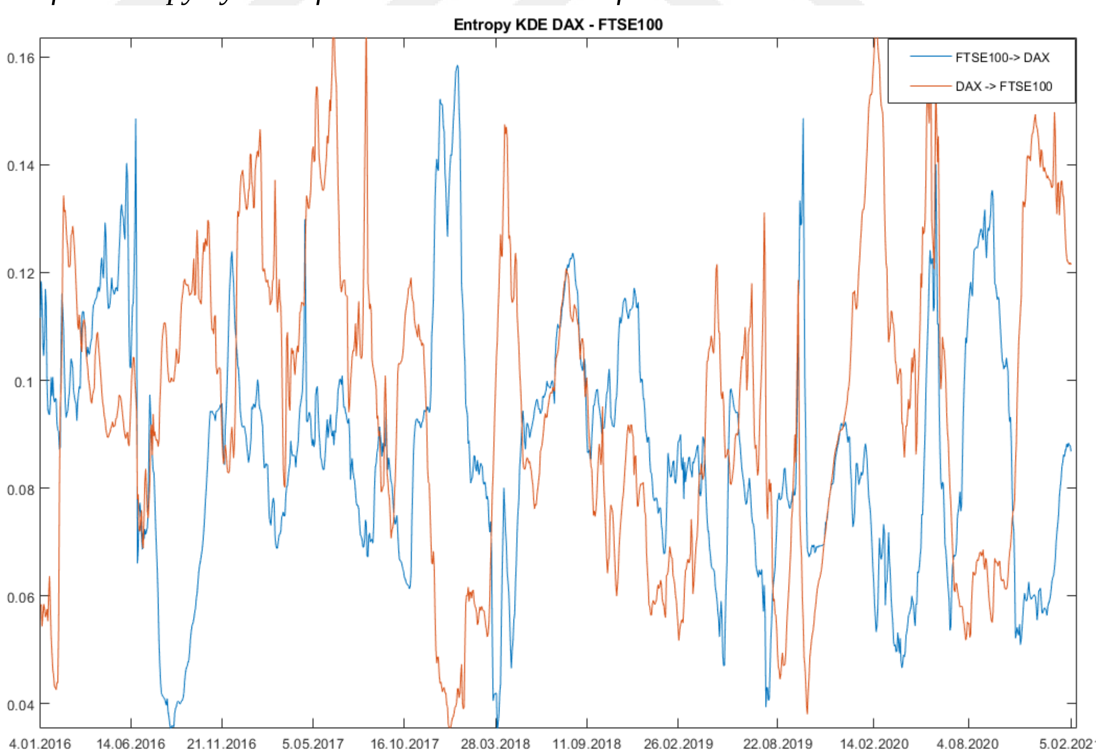

In a financial crisis, the financial time series show the same characteristics and they co-move in that periods. We studied the co-movement of stock indices by WTC and

Figure 24

1.WTC S&P500-DAX from 4.01.2016-5.02.2021, 2.TE of S&P500-DAX from 16.10.2017- 04.08.2020

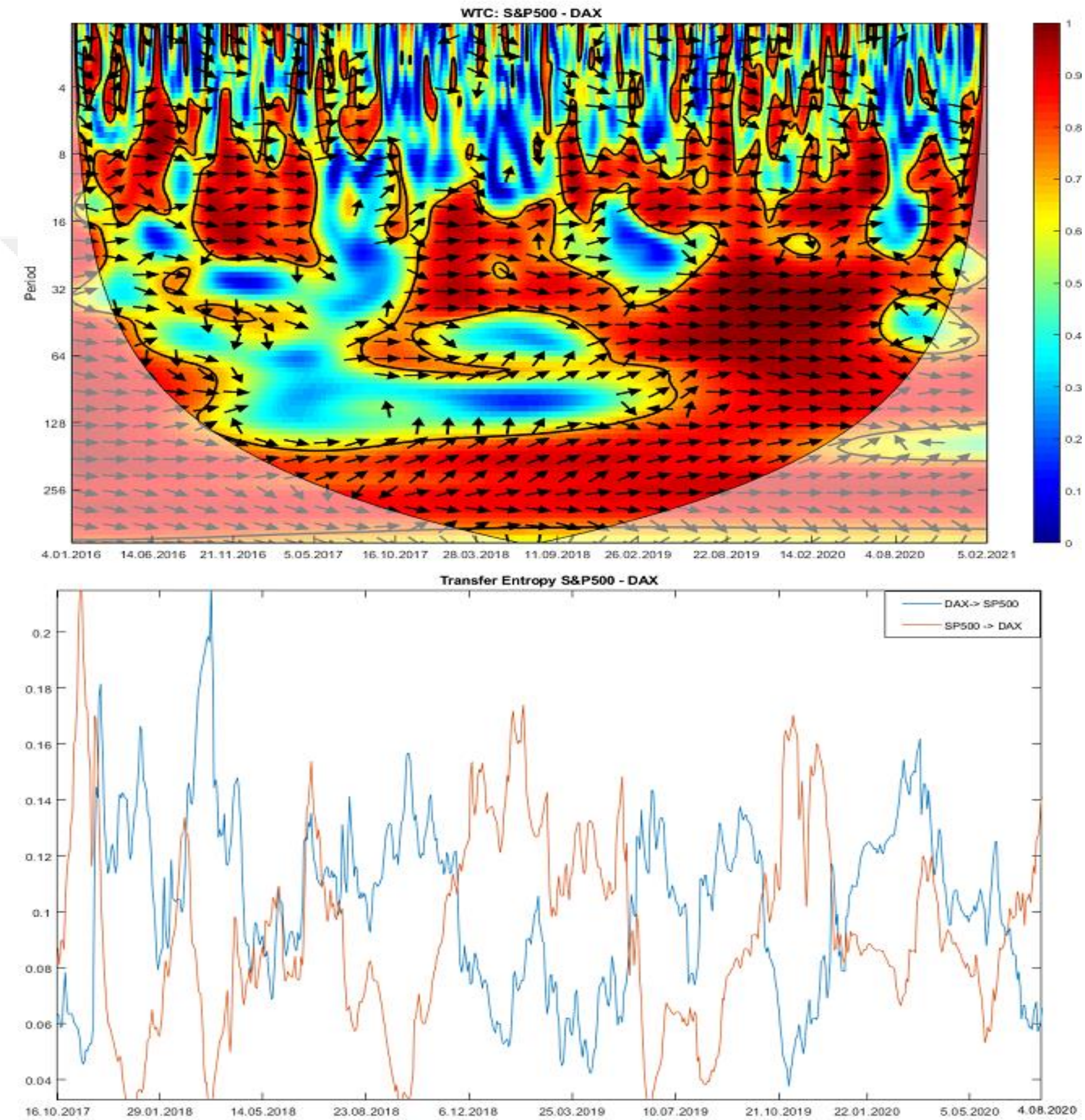

according to TE results we aim to show the information flow during the financial crisis period because we believe in financial shocks (coherence areas in WTC figures) the information flow is an important indicator for portfolio diversification and investing. We analyzed the WTC and TE of stock indices from Figure 24 to Figure 26, TE measures of them in corresponding coherence periods are presented in Table 9, the bold text gives higher TE values which explain the direction of information flow on given pair.

Figure 25

1.WTC S&P500-FTSE100 4.01.2016-5.02.2021, 2.TE of S&P500-FTSE100 7.11.2018-04.08.2020

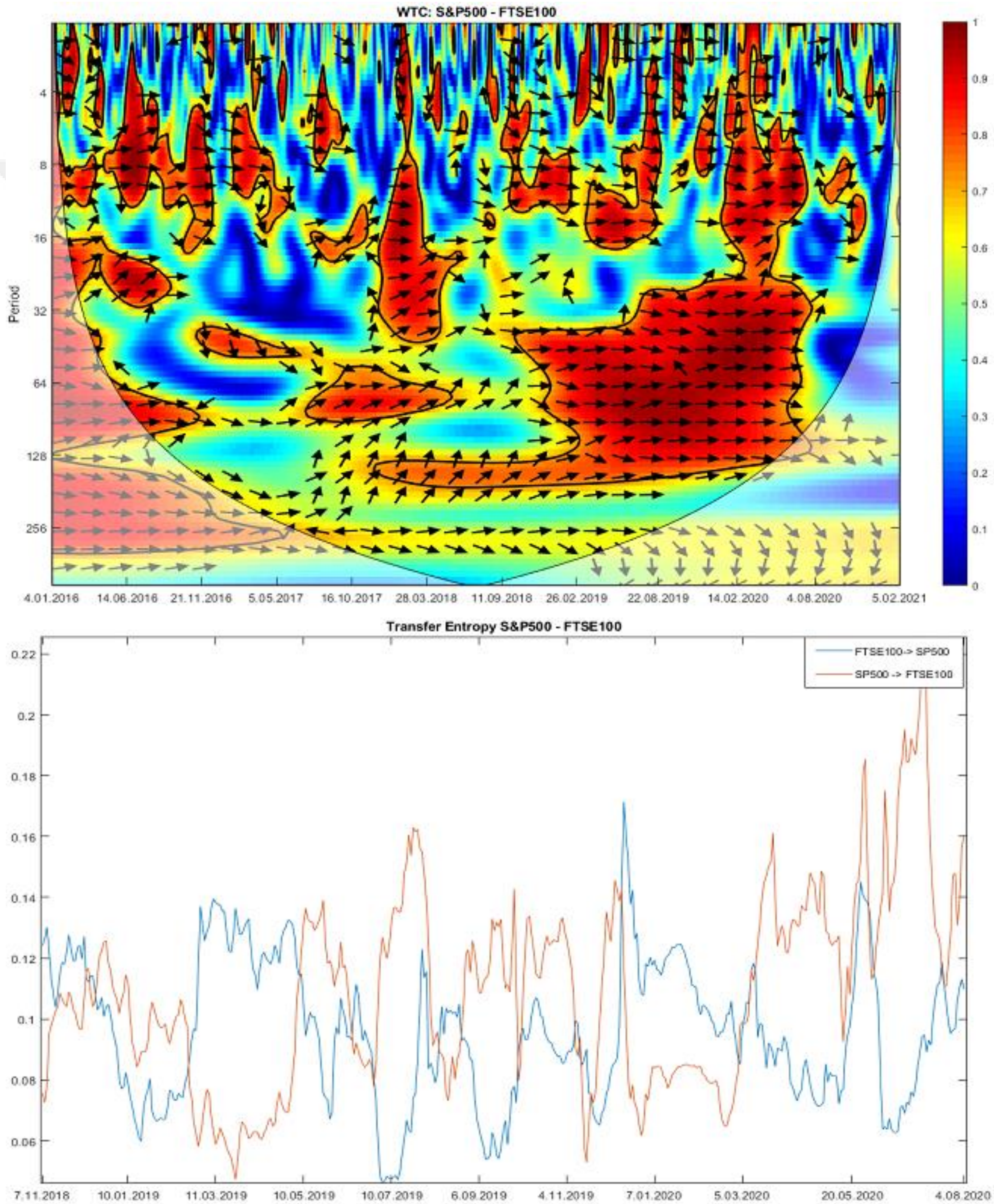

Table 9

Transfer Entropy Between Stock Indexes on Coherent Periods

Coherent Periods	Pair	
16.10.2017 – 4.08.2020	$TE_{SP500\text{->}DAX}$: 0.0934	**$TE_{DAX\text{->}SP500}$: 0.1020**
7.11.2018 – 4.08.2020	**$TE_{SP500\text{->}FTSE100}$: 0.1605**	$TE_{FTSE100\text{->}SP500}$: 0.1099
16.10.2017-22.10.2020	$TE_{DAX\text{->}FTSE100}$: 0.0763	**$TE_{FTSE100\text{->}DAX}$: 0.0818**

In Figure 24.1 the coherence dates between 16.10.2017- 04.08.2020 (dark red color areas), stock indices co-moved in these time intervals. These coherent periods were used to understand the information flows between stock indices by the Transfer Entropy KDE approach with the guidance of WTC. We can easily see that in Figure 24.2, in almost all time period $TE_{DAX\text{->}S\&500}$(blue line) is higher(above) than the $TE_{S\&P500\text{->}DAX}$ (red line) except time from 1.12.2018 to 1.05.2019, which means information flows is from DAX to SP500. The values in Table 9, show same results since $TE_{DAX\text{->}S\&500}$ =0.1020 > $TE_{S\&P500\text{->}DAX}$=0.0934. These results can be supported by the WTC figure since the arrow directions are almost upwards in all dates which denote that DAX is on the leading side when comparing S&P500.

In Figure 25.1, the coherence dates between 7.11.2018- 04.08.2020 (dark red color areas), stock indices co-moved in these time intervals. The arrows move right means indices are in phase and from 16.10.2017 to 10.05.2019 the arrows move up by approximately 90 degrees means FTSE100 leads S&P500 for this time interval, and after this time the arrow directions move downward with a small slope, so S&P500 dominates the FTSE100, this result supported by Figure 25.2, because before the date 10.05.2019 $TE_{FTSE100\text{->}S\&500}$(blue line) higher(above) than the $TE_{S\&P500\text{->}FTSE100}$(red line) and after this date the direction of information flow changes and SP500 dominates FTSE100 and also in Table 9, $TE_{SP500->FTSE100}$: 0.1605 > $TE_{FTSE100->SP500}$: 0.1099 indicate that net TE greater than zero so the above results are backed up again.

Figure 26

1.WTC DAX-FTSE100 from 4.01.2016-5.02.2021, 2.TE of DAX-FTSE100 from 16.10.2017- 22.10.2020

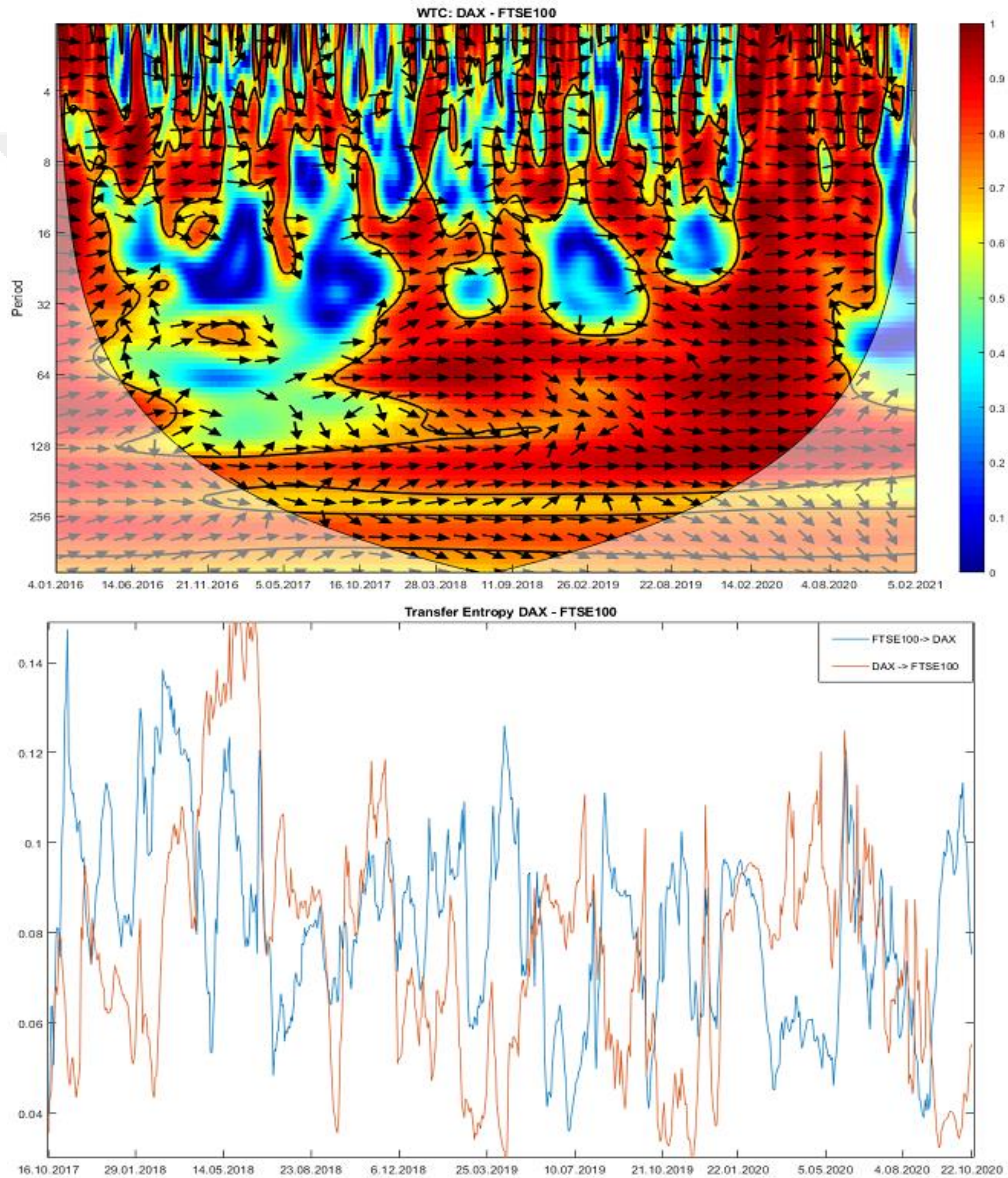

The red color areas which are shown in Figure 26.1, are the coherent dates between 16.10.2017 -22.10.2020. If we analyze the WTC of DAX and FTSE100, the arrow directions move right and up in almost all time frames indicate that they are in phase and there is causality from FTSE100 to DAX. The information flow between DAX and FTSE100, for coherent periods, is presented in Table 9 and Figure 26.2. Approximately for 3 year periods, $TE_{\mathbf{DAX->FTSE100}}$(blue line) higher (above) than the $TE_{\mathbf{FTSE100->DAX}}$ (red line) and the TE values in Table 9, $TE_{\mathbf{DAX->FTSE100}}$:0.0763< $TE_{\mathbf{FTSE100->DAX}}$: 0.0818 prove that information flow is from FTSE100 to DAX in the consistent time period analyzed from 16.10.2017 -22.10.2020. According to the results obtained in the two figures, we saw that the WTC and TE analyze gave similar results in the same periods.

According to the results of Table 9 and Figures 24, 25, 26, there exists a bidirectional information flow between stock indices, DAX to S&P500, S&P500 to FTSE100, and FTSE100 to DAX. Therefore, we concluded that for their coherent times, the causality between indices will be changed.

In the COVID period we faced the last financial crisis, for this reason, we also add this period to our TE measurement because we want to show the relation of stock indices in special crisis, COVID period, to give ideas for future outlooks. The results obtained by TE between stock indices on this period are presented in Table 10 and Figures 28, 29, 30, and daily prices of stock indices are shown in Figure 27 for the period 2.01.2020-30.06.2021.

Figure 27

Daily Prices of S&P500, DAX, and FTSE100 on COVID period from 2.01.2020 to 30.06.2021

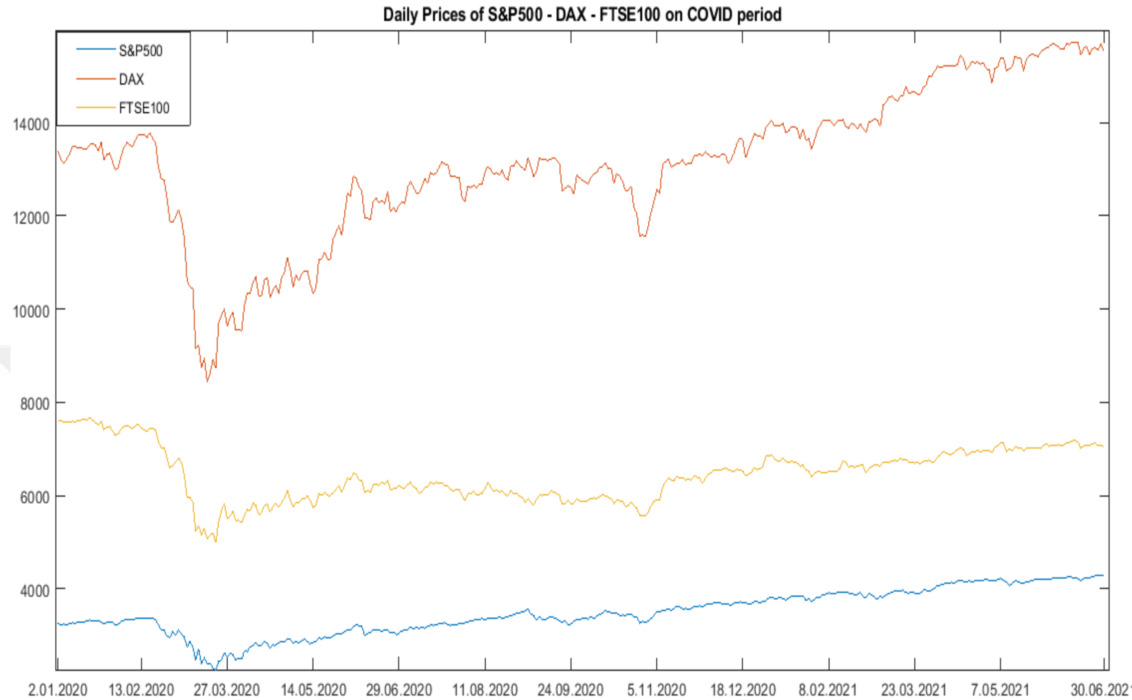

Table 10

Transfer Entropy Between Indexes on COVID Period from 02.01.2020 to 30.06.2021

	S&P500	DAX	FTSE100
S&P500	0	0.0659	**0.0879**
DAX	**0.1011**	0	**0.0620**
FTSE100	0.0843	0.0408	0

In Table 10, we interpreted TE values for every bidirectional pair on the COVID period measured row to column and bold text represents the higher TE values of one than the other. According to this, It is seen that DAX dominates other stock indices on the

COVID period obtained by WTC analysis. Also, there is more information flow to FTSE100 from DAX and S&P500.

Figure 28

Transfer Entropy of SP500 and DAX on COVID period from 2.01.2020 to 30.06.2021.

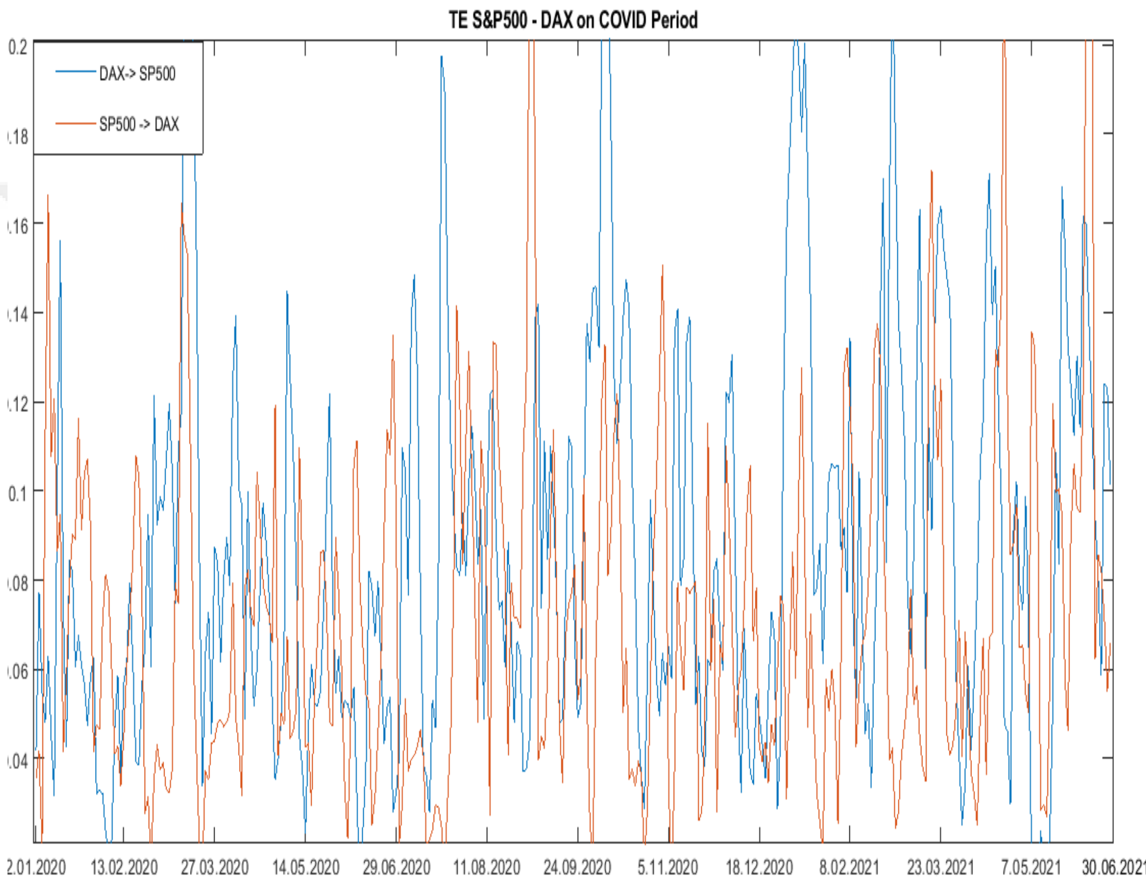

In Figure 28, we analyzed the TE between S&P500 and DAX from 2.01.2020 to 30.06.2021 and in Table 10, we obtained mutually supportive results. The information flow DAX to S&P500, since $TE_{DAX\text{->}S\&500}$(blue line) is higher (above) than the $TE_{S\&P500\text{->}DAX}$ (red line) except the beginning of COVID period and this will be as a result of earlier COVID cases in America and earlier measures taken in the economy than in Europe. In Table 10, TE values between them also give same outputs since $TE_{\mathbf{DAX\text{->}SP500}}$: 0.1011 > $TE_{\mathbf{SP500\text{->}DAX}}$: 0.0659, means DAX leads S&P500. If we compare with the WTC of S&P500 and DAX in Figure 24.1, for the COVID period, after the date 14.02.2020 the arrow directions almost upward also indicate that there is causality from DAX to S&P500.

Figure 29

TE of SP500 and FTSE100 on COVID period from 2.01.2020 to 30.06.2021.

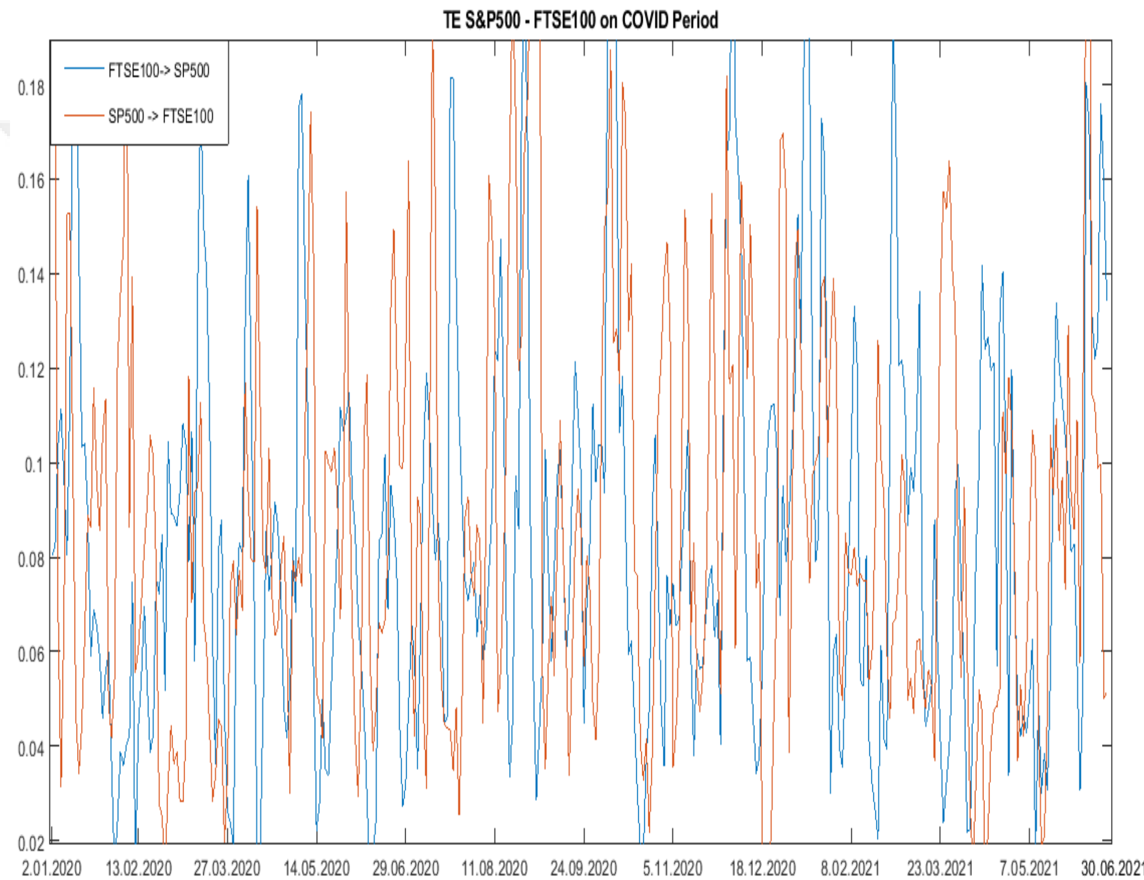

We interpreted the TE between S&P500 and FTSE100 on COVID period from 2.01.2020 to 30.06.2021 in Figure 29, and it is seen that there is an information flow S&P500 to FTSE100 since $TE_{S\&P500\text{->}FTSE100}$(red line) higher (above) than $TE_{FTSE100\text{->}S\&500}$(blue line). If we interpret it together with the results in Table 10, we will encounter similar conclusions, since $TE_{\mathbf{SP500\text{->}FTSE100}}$: 0.0879 > $TE_{\mathbf{FTSE100\text{->}SP500}}$:0.0843, means S&P500 leads FTSE100. If we look at the WTC of S&P500 and FTSE100 in Figure 25.1, the first date of the COVID period 02.01.2021 is inside the coherent period, the downward directions of arrows claim that S&P500 dominated FTSE100.

Figure 30

Transfer Entropy of DAX and FTSE100 on COVID period from 2.01.2020 to 30.06.2021.

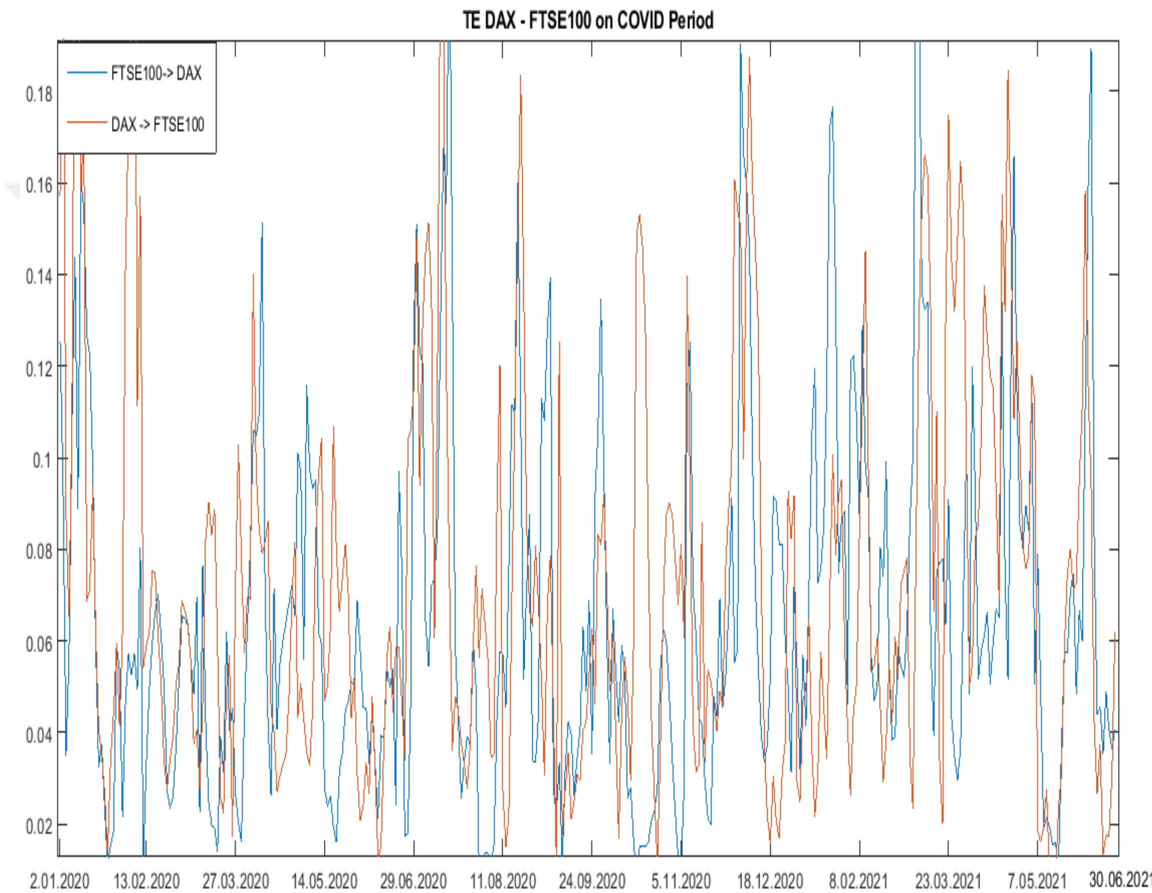

In Figure 30, there exists an information flow from DAX to FTSE100, since for the COVID period from 2.01.2020 to 30.06.2021 $TE_{DAX\text{->}FTSE100}$(red line) higher (above) than the $TE_{FTSE100\text{->}DAX}$ (blue line) and also in Table 10, we got similar results. $TE_{\mathbf{DAX\text{->}FTSE100}}$: 0.0620 > $TE_{\mathbf{FTSE100\text{->}DAX}}$: 0.0408, means DAX dominates FTSE100. In WTC of DAX and FTSE100 in Figure 26.1, we obtain overlapping results, because almost upward directions of arrows claim that there is causality from DAX to FTSE100.

The outcomes of Table 10 and Figures 28, 29 and 30, showed that there exist DAX dominates S&P500 and FTSE100 on COVID period. This may be a result of the fact that Germany has fewer cases of COVID-19 than in the United Kingdom and the United States. In the light of these analyzes, we can assume that the dynamics of the German economy are in a more robust structure during the COVID period.

3.5. Conclusion

In this chapter, we examine the co-movement of stock indices which are FTSE100 in the United Kingdom, the DAX in Germany, and the S&P500 Index in the United States through WTC, and information flow between them by TE. Here, we have stated that TE can detect the information flow in directional coupling between two stock indices. It can help us to see the direction of the net flow. WTC detects the financial crisis or coherence periods in the time-frequency domain and we interpreted rise and fall in the information transfer and direction of it during these periods by TE. After WTC analysis, coherence areas are used for TE measure. When we compare the WTC and TE figures we faced congruence results. WTC and TE outcomes support each other. When the arrow directions change in WTC figures, at the same time we see a change of direction in the lines on the TE graphs.

We used the KDE method for TE measure. We conclude that DAX was the most influential stock index and FTSE100 is the most dominated for 5 year period. During the coherence periods, bidirectional information flow was exist from DAX to S&P500, S&P500 to FTSE100, and FTSE100 to DAX, and on COVID period DAX took the information in firstly and dominated the others.

Two years ago, we faced the worst crisis ever which was COVID. Some Countries have experienced the worst financial and economic crises in their history. We have added this period to our thesis to predict what the behavior of stock indices might be in a similar situation in the coming years and to guide investors. In WTC figures we can easily see that all stock indices showed high co-movements in the first year of the COVID period and we also analyze the information flow in that time. According to results, DAX was in the leading position, and FTSE100 most dominated on the COVID period.

In conclusion, in this chapter three different results are obtained: 1) DAX is on the leading side in general for five year periods, 2) Bidirectional information flows for every pair on coherent periods and, 3) TE guided WTC analysis shows, TE sign change can be explained by phase angle direction got with WTC. WTEGTM allows us to capture the change in the causality and direction of net information flow between nonlinear and nonstationary time series simultaneously, especially in times of financial crisis like in the COVID period. These two methods give equivalent and correct outputs in coherence times. In the future, this method can be used to anticipate risk in times of crisis like COVID. Therefore, we interpret these results as the investors adjust their portfolio positions for stock indices in financial crisis periods.

4. DISCUSSIONS

The relationships between financial time series are a very important indicator in analyzing the economic shocks encountered. There are many methodologies and analyzes on this subject in the literature. The aim of the thesis is to analyze the co-movement of financial time series, fractal behavior, information flow, and future price forecasting, and to develop new analysis methods. In the first part of the thesis, the co-movement of financial time series was analyzed by Wavelet coherence (WTC) method, crisis and shock periods were determined by Multiple wavelet coherence (MWC) method, then fractal behaviors were examined with Multifractal de-trended fluctuation analysis (MFDFA) method and for the post-crisis periods, daily price range estimations for the future were made by using the Vector autoregressive fractionally integrated moving average (VARFIMA) method, in comparison with real data. As a result of the analysis, it was determined that the series with the highest fractal characteristics had a more reliable forecast range in the forecasting analyses made after the crisis periods when the detected co-movement was high. In the second part, a new method called Wavelet transform guided transfer entropy method (WTGTEM) has been proposed. In this new method, the co-movement of exchange rate time series has been examined with the Wavelet coherence (WTC) method, and the measurement and direction of the information flow between the financial series under the guidance of WTC have been analyzed by the Transfer entropy (TE) method. As a result of the analyzes made, it has been seen that both methods successfully explain the causality and relationship in crisis periods and provide consistent results. In the last part of the thesis, the new methodology presented in the second part has been applied to major stock indices. Especially during the COVID period, the behavior of the series has been analyzed. As a result of the analysis, it has been shown that the causality and relationship between the series during and before the COVID period were successfully detected in both methods, and it would be helpful for investors in portfolio diversification, especially in times of crisis. We believe that this thesis will guide future studies of this kind and that the methods used will be preferred by researchers.

REFERENCES

Barnett, L., Barrett, A. B., & Seth, A. K. (2009). Granger causality and transfer entropy are equivalent for Gaussian variables. *Physical review letters*, *103*(23), 238701.

Barunik, J., & Vacha, L. (2013). Contagion among Central and Eastern European stock markets during the financial crisis. *arXiv preprint arXiv:1309.0491*.

Barunik, J., Aste, T., Di Matteo, T., & Liu, R. (2012). Understanding the source of multifractality in financial markets. *Physica A: Statistical Mechanics and its Applications*, *391*(17), 4234-4251..

Batten, J., & Ellis, C. (1996). Fractal structures and naive trading systems: Evidence from the spot US dollar/Japanese yen. *Japan and the world economy*, *8*(4), 411-421.

Benoit, B. M. (1977). *Fractals: form, chance, and dimension*. W.H. Freemen & Company, San Francisco, CA.

Dias, G. F., & Kapetanios, G. (2014). *Forecasting medium and large datasets with Vector Autoregressive Moving Average (VARMA) models*. School of Economics and Management.

Falconer, K. (1990). *Fractal Geometry: Mathematical Foundations and Its Applications*. John Wiley & Sons.

Gherghina, Ș. C., & Simionescu, L. N. (2021). Exploring the co-movements between stock market returns and COVID-19 pandemic: evidence from wavelet coherence analysis. *Applied Economics Letters*, 1-9.

Goodell, J. W., & Goutte, S. (2021). Co-movement of COVID-19 and Bitcoin: Evidence from wavelet coherence analysis. *Finance Research Letters, 38*, 101625.

Granger, C. W. (1969). Investigating causal relations by econometric models and cross-spectral methods. *Econometrica: journal of the Econometric Society*, 424-438.

Grinsted, A., Moore, J. C., & Jevrejeva, S. (2004). Application of the cross wavelet transform and wavelet coherence to geophysical time series. *Nonlinear processes in geophysics*, *11*(5/6), 561-566.

Gunay, S. (2014). Source of the multifractality in exchange markets: multifractal detrended fluctuations analysis. *Journal of Business & Economics Research (JBER)*, *12*(4), 371-384.

He, J., & Shang, P. (2017). Comparison of transfer entropy methods for financial time series. *Physica A: Statistical Mechanics and its Applications*, *482*, 772-785.

Ihlen, E. A. F. E. (2012). Introduction to multifractal detrended fluctuation analysis in Matlab. *Frontiers in physiology*, *3*, 141.

Jiang, Y., Yu, M., & Hashmi, S. M. (2017). The financial crisis and co-movement of global stock markets—A case of six major economies. *Sustainability*, *9*(2), 260.

Kaiser, A., & Schreiber, T. (2002). Information transfer in continuous processes. *Physica D: Nonlinear Phenomena*, *166*(1-2), 43-62.

Karatas, C., & Unal, G. (2021). Co-movement, fractal behaviour and forecasting of exchange rates. *International Journal of Dynamics and Control*, *9*(4), 1818-1831.

Karatas, C., Unal, G., & Yilmaz, A. (2017). Co-movement and forecasting analysis of major real estate markets by wavelet coherence and multiple wavelet coherence. *Chinese Journal of Urban and Environmental Studies*, *5*(02), 1750010.

Lee, J., Nemati, S., Silva, I., Edwards, B. A., Butler, J. P., & Malhotra, A. (2012). Transfer entropy estimation and directional coupling change detection in biomedical time series. *Biomedical engineering online*, *11*(1), 1-17.

Leland, W. E., Taqqu, M. S., Willinger, W., & Wilson, D. V. (1994). On the self-similar nature of Ethernet traffic (extended version). *IEEE/ACM Transactions on networking*, *2*(1), 1-15.

Lütkepohl, H. (2006). Forecasting with VARMA models. *Handbook of economic forecasting*, *1*, 287-325.

Lütkepohl, H., & Poskitt, D. S. (1998). Consistent estimation of the number of cointegration relations in a vector autoregressive model. In *Econometrics in theory and practice* (pp. 87-100). Physica-Verlag HD.

Mendoza Urdiales, R. A., García-Medina, A., & Nuñez Mora, J. A. (2021). Measuring information flux between social media and stock prices with Transfer Entropy. *PloS one*, *16*(9), e0257686.

Mohaghegh, A., Hamidiyan, M., Hosseini Esfidvajani, S. A., & Jafari, G. (2021). Investigating the Financial Crisis of the Iranian Stock Exchange Using Transfer Entropy Method and comparing it with the Dow Jones Financial Market. *Propósitos Y Representaciones. Journal of Educational Psychology*, 9(SPE1), e886. https://doi.org/10.20511/pyr2021.v9nSPE1.886

Mulligan, R. F. (2004). Fractal analysis of highly volatile markets: an application to technology equities. *The quarterly review of economics and finance*, *44*(1), 155-179.

Olayeni, O. R. (2016). Causality in continuous wavelet transform without spectral matrix factorization: theory and application. *Computational Economics*, *47*(3), 321-340.

Onali, E., & Goddard, J. (2011). Are European equity markets efficient? New evidence from fractal analysis. *International review of financial analysis*, *20*(2), 59-67.

Ongan, S., & Gocer, I. (2017). Testing the causalities between economic policy uncertainty and the US stock indices: Applications of linear and nonlinear approaches. *Annals of Financial Economics*, *12*(04), 1750016.

Özdurak, C., & Karataş, C. (2021). Covid-19 and the Technology Bubble 2.0: Evidence from DCC-MGARCH and Wavelet Approaches. *Journal of Applied Finance and Banking*, *11*(2), 109-127.

Park, S., Jang, K., & Yang, J. S. (2021). Information flow between bitcoin and other financial assets. *Physica A: Statistical Mechanics and its Applications*, *566*, 125604.

Parzen, E. (1962). On estimation of a probability density function and mode. *The annals of mathematical statistics*, *33*(3), 1065-1076.

Peters, E. E. (1994). *Fractal market analysis: applying chaos theory to investment and economics* (Vol. 24). John Wiley & Sons.

Richards, G. R. (2000). The fractal structure of exchange rates: measurement and forecasting. *Journal of International Financial Markets, Institutions and Money*, *10*(2), 163-180.

Rosenblatt, M. (1956). Remarks on some nonparametric estimates of a density function. *Annals of Mathematical Statistics*. 27 (3): 832–837. doi:10.1214/aoms/1177728190

Schreiber, T. (2000). Measuring information transfer. *Physical review letters*, *85*(2), 461.

Sensoy, A., Sobaci, C., Sensoy, S., & Alali, F. (2014). Effective transfer entropy approach to information flow between exchange rates and stock markets. *Chaos, solitons & fractals*, *68*, 180-185.

Shannon, C. E. (1948). A mathematical theory of communication. *The Bell system technical journal*, *27*(3), 379-423.

Sumioka, H., Yoshikawa, Y., & Asada, M. (2007, July). Causality detected by transfer entropy leads acquisition of joint attention. In *2007 IEEE 6th international conference on development and learning* (pp. 264-269). IEEE.

Teng, Y., & Shang, P. (2017). Transfer entropy coefficient: Quantifying level of information flow between financial time series. *Physica A: Statistical Mechanics and its Applications*, *469*, 60-70.

Tiwari, A. K. (2012). Decomposing time-frequency relationship between interest rates and share prices in India through wavelets.

Torrence, C., & Compo, G. P. (1998). A practical guide to wavelet analysis. *Bulletin of the American Meteorological society*, *79*(1), 61-78.

Vacha, L., & Barunik, J. (2012). Co-movement of energy commodities revisited: Evidence from wavelet coherence analysis. *Energy Economics*, *34*(1), 241-247.

Ver Steeg, G., & Galstyan, A. (2012, April). Information transfer in social media. In *Proceedings of the 21st international conference on World Wide Web* (pp. 509-518).

Yao, C. Z., & Li, H. Y. (2020). Effective transfer entropy approach to information flow among epu, investor sentiment and stock market. *Frontiers in Physics*, *8*, 206.

Yilmaz, A., Unal, G., & Karatas, C. (2017). Wavelet Based Analysis of Major Real Estate Markets. *Journal Of Advanced Studies In Finance*, *7*(2), 107-116.

Appendix A List of Abbreviations

- WTC - Wavelet Coherence
- MWC – Multiple Wavelet Coherence
- MF-DFA - Multifractal De-trended Fluctuation Analysis
- VARFIMA - Vector Autoregressive Fractionally Integrated Moving Average
- CWT - Continuous Wavelet Transform
- XWT – Cross Wavelet Transform
- H – Hurst Exponent
- R/S – Rescaled Range
- TE – Transfer Entropy
- KDE – Kernel Density Estimation
- EPU – Economic Policy Uncertainty
- WTGTEM – Wavelet Transform Guided Transfer Entropy Method
- RMS – Root Mean Square

Appendix B List of Symbols

- $W_x(\tau, s)$ - Continuous Wavelet Transform
- $\varphi(\eta) -$ Morlet Wavelet
- $W_n^X(s) -$ Wavelet Transform
- $\Psi_n^{XY}(s) -$ Cross Wavelet Transform
- $R_n^2(s) -$ Wavelet Coherence
- $\varphi_{xy}(u, s) -$ Phase difference
- $R^2_{1(2,3,\dots,p)}$ – Multiple Wavelet Coherence
- $F_q(n) -$ The function of q^th order fluctuation
- Δh $-$ The scale of multifractality
- d - differencing degree
- H(x) – Shannon Entropy
- MI(X;Y) – Mutual Information
- $K(r)$ - Gaussian Kernel
- $T_{Y \rightarrow X} -$ Information Flow From Y to X.
- $P(x_k) -$ probability of x_k .